

Hybrid genetic dragonfly algorithm based optimal power flow for computing LMP at DG buses for reliability improvement

Venkataramana Veeramsetty¹ · Chintham Venkaiah¹ ·
D. M. Vinod Kumar¹

Received: 12 May 2017 / Accepted: 11 December 2017 / Published online: 21 December 2017
© Springer-Verlag GmbH Germany, part of Springer Nature 2017

Abstract This paper proposes an hybrid method to compute locational marginal price at distributed generation (DG) buses in order to improve reliability in radial distribution system (RDS). This method consists of optimal power flow based on hybrid genetic dragonfly algorithm which provides incentives to each DG unit based on its contribution to reliability improvement. In this paper expected energy not supplied has been used as a reliability measuring index. The proposed method enables the distribution company (DISCO) to operate the network with more reliability by providing proper incentives to DG owners. The proposed method has been implemented on 38 bus RDS and pacific gas and electric company (PG&E) 69 bus RDS under MATLAB environment. It has been observed from the analytical study on both test systems that by providing proper incentives to DG units, reliability of the network can be vastly improved.

Keywords Locational marginal price (LMP) · Distributed generation (DG) · Reliability · Expected energy not supplied (EENS) · Genetic algorithm · Dragonfly algorithm · Hybrid genetic dragonfly algorithm

✉ Venkataramana Veeramsetty
vvr.nitw@ieee.org

Chintham Venkaiah
ch.venkaiah@ieee.org

D. M. Vinod Kumar
vinodkumar.dm@gmail.com

¹ Department of Electrical Engineering, NIT Warangal, Hanamkonda, India

Nomenclature

ω_{inv} , ω_{emis} , ω_{los}	Weights corresponding to DISCO's investment, emission and loss respectively
ω_i	Weight corresponding to type 'i' loads
a_i , b_i , c_i	Fuel cost coefficients of DG unit i
AL_i	Actual load supplying to all type i buses in kW
AL_i^{LL}	Lower limit of actual load supplying to all type i buses
AL_i^{UL}	Upper limit of actual load supplying to all type i buses
$DISCO_{inv}^{part-II}$	DISCO's investment to purchase power from DG units in part-II of network in \$
$DISCO_{inv}^{part-I}$	DISCO's investment to purchase power from grid and DG units in part-I of network in \$
$DISCO_{max}^{inv}$	DISCO's investment to purchase maximum power from DG units in part-II of network in \$
$EENS_{base}^l$	EENS value due to outage of line 'l' under base case
$EENS_l$	EENS value due to outage of line l with DG
$EENS_l^{norm}$	Normalized EENS value due to outage of line l with DG
$Emis^{part-II}$	Emission released from part-II of network in kg
$Emis^{part-I}$	Emission released from part-I of network in kg
$Emis_{max}^{part-II}$	Maximum emission released from part-II of network in kg
LD_{ren}	Matrix which has line and bus information of part-I of network after renumbering
LD_{sub}	Matrix which has line and bus information of part-I of network
LD_{ws}	Matrix which has line and bus information of part-II of network
LD_{ws}^{ren}	Matrix which has line and bus information of part-II of network after renumbering
$Line_{out}$	Outaged line
LMP_i	LMP value of DG unit i
$LMP_i^{R_b}$	LMP value of DG unit i which is located at bus ' R_b '
$Loss^{part-II}$	Active power loss in part-II of network
$Loss^{part-I}$	Active power loss in part-I of network
$Loss_{max}^{part-II}$	Base case active power loss in part-II of network
LP_{ws}	Vector having sending end nodes of each line in part-II of network
LQ_{ws}	Vector having receiving end nodes of each line in part-II of network
n	Number of buses in network
$N_{DG}^{part-II}$	Number of DG units in part-II of network
n_{line}	Number of lines in network
n_{sub}	Number of buses in part-I of network
$N_{type}^{part-II}$	Different type of buses in part-II of network
n_{ws}	Number of buses in part-II of network
$nline_{sub}$	Number of lines in part-I of network
$nline_{ws}$	Number of lines in part-II of network
$Node_{Sorted}^{part-I}$	Matrix containing all buses in part-I of network in ascending order

P_{gen}^i	Scheduled generation of DG unit i in kW
$P_{gen}^i(R_b)$	Scheduled active power of DG unit ' i ' which is located at bus ' R_b '
$P_{gen}^{LL}(i)$	Lower generation limit of DG unit i
$P_{gen}^{max}(R_b)$	Maximim capacity of DG unit which is located at bus ' R_b '
$P_{gen}^{UL}(i)$	Upper generation limit of DG unit i
P_{Load}^{Act}	Vector having actual loads at each bus
$P_{Load}^{Alloc}(i)$	Allocated load to each bus i
P_{Load}^{Com}	Total commercial load in part-II of network
P_{Load}^{Ind}	Total industrial load in part-II of network
P_{Load}^i	Active power load at bus i
P_{Load}^{Mod}	Vector having modified loads at each bus
$P_{load}^{part-II}$	Total active power load in part-II of network
P_{load}^{part-I}	Total active power load in part-I of network
P_{Load}^{Res}	Total residential load in part-II of network
P_{min}	Minimum withdrawal of active power
P_{Bus}^{min}	Bus which has minimum withdrawal active power
P_{net}^i	Net active power load at bus i
R_b	Receiving end bus of outage line
S_l	Apparent power flowing through line l
S_l^{max}	Thermal limit of line l
TL_i	Total load at all type i buses in kW
V_i	Voltage at bus i
V_i^{LL}	Lower limit for voltage at bus i
V_i^{UL}	Upper limit for voltage at bus i
$CO_2^{DG_i}$	CO_2 released by DG unit i (kg/MW)
CO_2^{sub}	CO_2 released based on load at substation bus (kg/MW)
CO^{DG_i}	CO released by DG unit i (kg/MW)
CO^{sub}	CO released based on load at substation bus (kg/MW)
$NO_x^{DG_i}$	NO_x released by DG unit i (kg/MW)
NO_x^{sub}	NO_x released based on load at substation bus (kg/MW)
$SO_2^{DG_i}$	SO_2 released by DG unit i (kg/MW)
SO_2^{sub}	SO_2 released based on load at substation bus (kg/MW)
LP	Vector having sending end nodes of each line
LQ	Vector having receiving end nodes of each line

1 Introduction

The distribution networks are prone to failure [1] and hence the supply from power generation plants to the distribution networks will be interrupted [2,3]. Statistics emphasize the necessity of reassessment of available strategies to improve the electrical services by improving reliability of network [4].

Most of the radial distribution systems (RDSs) have been operated in a radial structure as the operation is simple and coordinating the protecting devices can be

easy. In order to improve reliability, loop systems concept has been introduced to support uninterrupted power flow to the load by including the inherent complexity of coordinating simple protection devices [5].

Some of the most significant methods [6–8] to improve reliability of the system are as follows:

- Adding protective devices
- Having fewer equipment failures to avoid contingency
- Improving the accuracy of available protection methods
- Re-closing and switching
- Network automation
- Fast fault prediction techniques
- Fast team to accelerate the repair process
- Reconfiguration

In the last decade, the penetration of distributed generation resources in distribution network has increased globally. The main reasons [9, 10] for increasing the penetration are as follows:

- Reliability improvement
- Emission reduction
- Improvement of electrical distribution network reinforcement horizon
- Energy resources optimization
- Supply for future load demand
- Service quality
- Utilization of non-conventional energy resources
- Loss reduction
- Avoiding the investment in large power plants and transmission lines
- Voltage support

DG units can serve the loads of radial distribution system (RDS) during planned and unplanned network outages [11]. Islanding operation improves system reliability by preventing the loss of load during outage period. Thus when any outage occurs either due to maintenance or failure, formation of islands will improve system reliability [12].

In deregulated electricity market environment, DISCO Decision Maker (DM) needs to take technical decisions like deployment of DG and taking decisions that make economic sense like development of retail competition. DISCO's DM role is very important for the efficient operation from a technical and financial point of view as these decisions improve market operation like competition and technical operations like reliability and service quality [13].

With the integration of DG units, distribution network has been transformed from passive state to active state as in transmission network. A few operating methods like nodal pricing [14] which are employed in transmission network in deregulated environment could also be applied in active distribution network. Nodal pricing is one of the mechanisms for financial incentive used by DISCO to control privately owned DG units and to encourage DG owners to carry out technical decisions [15]. Locational

Table 1 Comparison of LMP computation features

Research contribution	Different features addressed by researchers						Approach
	A	B	C	D	E	F	
[14]	✓		✓				Marginal loss coefficients
[17]	✓		✓				Reconciliated marginal loss coefficients
[18]	✓		✓	✓			Power flow sensitivities
[19]	✓		✓		✓		Genetic algorithm
[15]	✓		✓				Shapley value method
[13]	✓	✓	✓				Nucleolus theory
[20]	✓	✓	✓				Nucleolus theory and 2-point estimation
[21]	✓	✓	✓				Shapley value and 2-point estimation
Proposed method	✓	✓	✓	✓	✓	✓	Hybrid genetic dragonfly algorithm (HGDA)

marginal price (LMP) is the most effective method to determine nodal price in practice [16].

Several researchers have addressed the different features of LMP computation in RDS and their contributions have been listed in Table 1.

- A: Loss reduction
- B: Emission reduction
- C: Changing DG benefit
- D: Congestion
- E: Voltage limits
- F: Reliability improvement

None of the researchers have addressed the issue of reliability improvement by computing LMP so far. When any line outage occurs due to either failure or maintenance [22] then the network splits into two parts. Part-I corresponds to network connected to substation whereas part-II corresponds to network disconnected from substation. There is no encouragement to DG owners from DISCO for supplying the load in part-II of the network.

In addition to the above, Mixed integer linear programming model [23] was developed for volt/var control and energy loss minimization in electric power distribution network with DG units. It also provides optimal solution for placement of capacitor banks by considering energy loss, voltage deviation and acquisition, installation and maintenance costs of capacitors as objectives. Another mixed integer linear programming model has been proposed in [24] to solve the short term expansion problem in RDS. The solutions which were considered for this problem are construction/reconductoring of circuits and allocation of capacitor banks and voltage regulators. These two methodologies provide valuable contribution to improve operation of electric power RDS. However the authors have not discussed about incentives provided to private DG owners in terms of LMP in RDS.

The problems related to RDS planning are non linear, non-convex, non-differentiable and constrained optimization problems with integer and continuous decision variables. Conventional optimization techniques have some flaws like curse of dimensionality and non-differentiability [25]. In addition to these, conventional techniques usually suffer from the problem of convergence at local minimum instead of at global. Hence these methods are not suggestible for solving problems which have a large number of local minimum points. Whereas heuristic and evolutionary algorithms are powerful and effective for solving complex real time problems [26]. Genetic algorithm (GA) simultaneously evaluates more number of points in search space and is most effective among existing evolutionary algorithms. Authors in [27] proposed a new swarm algorithm called dragonfly algorithm (DA) based on swarming behavior of dragonfly for hunting and migration.

In this paper hybrid genetic dragonfly algorithm (HGDA) based optimal power flow (OPF) has been proposed to compute LMP at DG buses for reliability improvement. In the proposed method, the state of the part-II of the network can be observed by computing LMP at each DG bus. It is assumed that, LMP at DG bus in the part-I of the network will be at market price.

The proposed method enables DISCO to plan for scheduling the load or the generation in part-II of the network. Load scheduling is being done if load is more than the available generation in part-II of network else generation scheduling is initiated. The proposed method provides generation and LMP for each DG unit and load that can be supplied at each bus in part-II of the network.

In the proposed method, the weighted sum of expected energy not supplied (EENS) for each type of bus in part-II of network has been considered as objective for load scheduling. However the weighted sum of objectives like DISCO's investment to purchase power from DG owners, emission and loss in part-II of network has been considered as single objective function for generation scheduling.

The original contributions of this paper are as follows:

- Considered LMP computation for improving the reliability for the first time
- Employed hybridization of the GA and DA for improved results for the first time
- Enabled DISCO's Decision Maker to handle tradeoff among the customers
- Enabled DISCO's Decision Maker to handle tradeoff among objectives like DISCO's investment cost, emission and active power loss during generation scheduling
- Estimate the state of the network with single contingency
- Developed algorithms to locate the buses beyond each line and to renumber the buses in both parts of the network

The remainder of the paper has been organized as follows. Section 2 presents problem formulation. Section 3 presents methodology used to compute LMP at DG buses. Section 4 reports the analysis of simulated results and Sect. 5 provides conclusion of this paper.

2 Problem formulation

The main aim of optimal power flow is either to schedule the load in case the total load is more than available generation or to schedule the generation in case the available generation is more than load in part-II of network. It is assumed that LMP at DG buses in the part-I of the network will be at market price. Generation of each DG unit ' i ' is computed as shown in Eq. (1) such that the DG owner will receive maximum profit at a given LMP. The bus which has more injection in part-II of the network is considered as slack bus. Slack bus position will not change during load scheduling. The position of slack bus may shuffle between DG buses in part-II of network during generation scheduling. If there exists only one DG unit whose generation is more than the local load then the DG unit bus is considered as a slack bus.

$$P_{gen}^i = \frac{LMP_i - b_i}{2a_i}. \quad (1)$$

2.1 Load scheduling

The optimal power flow is trying to optimize an objective by controlling power flow within an electrical network without violating network power flow constraints or system and equipment operating limits [28]. Minimization of Expected Energy Not Supplied (EENS) is considered as an objective function for load scheduling. In order to improve the reliability of network, all loads have to be served with out interruption. Reliability of RDS has been evaluated in terms of several indices such as System Average Interruption Frequency Index (SAIFI), System Average Interruption Duration Index (SAIDI) and Customer Average Interruption Duration Index (CAIDI). These indices are more helpful in operational perspective rather than planning [29] and are not adequate to evaluate reliability of industrial and commercial RDSs [30]. In this paper EENS [31] has been considered as network reliability evaluation parameter. Objective and fitness functions are as represented in Eqs. (2) and (3) respectively.

$$\begin{aligned} \min EENS_l &= \sum_{i=1}^{N_{type}^{part-II}} \omega_i * (TL_i - AL_i) * OT_l \\ \min EENS_l^{norm} &= \sum_{i=1}^{N_{type}^{part-II}} \omega_i * \frac{(TL_i - AL_i) * OT_l}{TL_i * OT_l} \\ &\quad i = 1 : \text{Residential Loads} \\ &\quad i = 2 : \text{Commercial Loads} \\ &\quad i = 3 : \text{Industrial Loads} \end{aligned} \quad (2)$$

$$\max \text{Fitness Function} = \frac{1}{1 + EENS_l^{norm}} \quad (3)$$

Subject to the following equality and inequality constraints as in Eq. (4).

$$\begin{aligned}
 & \sum_{i=1}^{N_{DG}^{part-II}} P_{gen}^i - \sum_{i=1}^{N_{type}^{part-II}} AL_i - Loss^{part-II} \approx 0 \\
 & \text{Voltage limits: } V_i^{LL} \leq V_i \leq V_i^{UL} \\
 & \text{Thermal limits: } S_l \leq S_l^{max} \\
 & \text{Load limits: } AL_i^{LL} \leq AL_i \leq AL_i^{UL}.
 \end{aligned} \tag{4}$$

AL_i^{UL} value depends on maximum capacity of DG units (P_{gen}^{max}) which are located on type i buses and TL_i . Assume bus 'b' is type 'i'. If the maximum capacity of DG unit (P_{gen}^{max}) is more than the load on the bus 'b' where it is located then AL_i^{UL} and TL_i are updated using Eq. (5) else using Eq. (6) by setting AL_i^{LL} always to zero.

$$\begin{aligned}
 AL_i^{UL} &= TL_i - P_{Load}^b \\
 TL_i &= TL_i - P_{Load}^b \\
 AL_i^{UL} &= TL_i - P_{gen}^{max} \\
 TL_i &= TL_i - P_{gen}^{max}
 \end{aligned} \tag{5} \tag{6}$$

Let P_{Load}^{Act} be vector which represents load on each bus of network containing 'n' number of buses as in Eq. (7). If the maximum capacity of DG unit (P_{gen}^{max}) is more than the load on bus 'i' where it is located then modify load on that bus 'i' using Eq. (8) else modify load on that bus 'i' using Eq. (9).

$$P_{Load}^{Act} = \{P_{Load}^1, P_{Load}^2, \dots, P_{Load}^i, \dots, P_{Load}^n\} \tag{7}$$

$$P_{Load}^{Mod} = \{P_{Load}^1, P_{Load}^2, \dots, P_{Load}^i = 0, \dots, P_{Load}^n\} \tag{8}$$

$$P_{Load}^{Mod} = \{P_{Load}^1, P_{Load}^2, \dots, P_{Load}^i = P_{Load}^i - P_{gen}^{max}, \dots, P_{Load}^n\} \tag{9}$$

The various type of loads considered in this paper are *residential loads*, *commercial loads* and *industrial loads*. Length of variable string depends on number of variables. If part-II of network contains all type of loads then $N_{type}^{Part-II} = 3$ and variable string is as shown in Eq. (10). Initial value of each element in variable string is randomly generated. This randomly generated loads were allocated proportionally among buses in part-II of network using Eqs. (11), (12), and (13).

$$\{P_{Load}^{Res}, P_{Load}^{Com}, P_{Load}^{Ind}\}. \tag{10}$$

If bus 'i' is a residential load bus then

$$P_{Load}^{Alloc}(i) = \frac{P_{Load}^{Mod}(i)}{TL_1} P_{Load}^{Res}. \tag{11}$$

If bus 'i' is a commercial load bus then

$$P_{Load}^{Alloc}(i) = \frac{P_{Load}^{Mod}(i)}{TL_2} P_{Load}^{Com}. \quad (12)$$

If bus 'i' is a industrial load bus then

$$P_{Load}^{Alloc}(i) = \frac{P_{Load}^{Mod}(i)}{TL_3} P_{Load}^{Ind}. \quad (13)$$

If the maximum capacity P_{gen}^{max} of DG unit is more than the load on bus 'i' where DG is located then $P_{load}^{Alloc}(i)$ is modified using Eq. (14) else $P_{load}^{Alloc}(i)$ is modified using Eq. (15).

$$P_{load}^{Alloc}(i) = P_{load}^{Alloc}(i) + P_{Load}^i \quad (14)$$

$$P_{load}^{Alloc}(i) = P_{load}^{Alloc}(i) + P_{gen}^{max}. \quad (15)$$

LMP at each DG bus where DG unit i is located in part-II of network is computed using Eq. (16) so that the DG owner receives maximum profit to generate P_{gen}^i .

$$LM P_i = 2a_i P_{gen}^i + b_i. \quad (16)$$

2.2 Generation scheduling

Generation scheduling has been opted for if the total load is less than available generation in part-II of network. The objective function and constraints which have been considered for generation scheduling are shown in Eqs. (17) and (18) respectively.

$$\min Obj = \omega_{inv} \frac{DISCO_{inv}^{part-II}}{DISCO_{max}^{inv}} + \omega_{emis} \frac{Emis^{part-II}}{Emis_{max}^{part-II}} + \omega_{los} \frac{Loss^{part-II}}{Loss_{max}^{part-II}} \quad (17)$$

$$Power\ balance : \sum_{i=1}^{N_{DG}^{part-II}} P_{gen}^i - P_{load}^{part-II} - Loss^{part-II} \approx 0$$

$$Generation\ limits : P_{gen}^{LL}(i) \leq P_{gen}^i \leq P_{gen}^{UL}(i)$$

$$Voltage\ limits : V_i^{LL} \leq V_i \leq V_i^{UL}$$

$$Thermal\ limits : S_l \leq S_l^{max}$$

(18)

P_{gen}^{LL} of DG depends on load on the bus where it is located. Assume DG unit i is located at bus 'b' then $P_{gen}^{LL}(i)$ and $P_{gen}^{UL}(i)$ are determined from the limits represented in Table 2.

Table 2 Limits on DG generation

Condition	$P_{gen}^{LL}(i)$	$P_{gen}^{UL}(i)$
$P_{Load}^b \leq P_{gen}^{max}(i)$	P_{Load}^b	$P_{gen}^{max}(i)$
$P_{gen}^{max}(i) \leq P_{Load}^b$	$P_{gen}^{max}(i)$	$P_{gen}^{max}(i)$

$DISCO_{inv}^{part-II}$ and $DISCO_{max}^{inv}$ have been computed based on cost coefficients of DG units using Eq. (19). Similarly, emission from part-I and part-II of network have been computed using Eqs. (20) and (21) respectively. However $Loss^{part-II}$ and $Loss_{max}^{part-II}$ are computed using backward and forward sweep load flow method [32]. This algorithm utilizes complete advantage of ladder structure of distribution network to achieve high speed, robust convergence and low memory requirements [33, 34]. In this load flow solution, a simultaneously controlled PQ modeled [35] DG has been used.

$$DISCO_{inv}^{part-II} = \sum_{i=1}^{N_{DG}^{part-II}} (2 * a_i * P_{gen}^i + b_i) * P_{gen}^i$$

$$DISCO_{max}^{inv} = \sum_{i=1}^{N_{DG}^{part-II}} (2 * a_i * P_{gen}^{max}(i) + b_i) * P_{gen}^{max}(i) \quad (19)$$

$$Emis^{part-I} = \sum_{i=1}^{N_{DG}^{part-I}} (SO_2^{DG_i} + CO_2^{DG_i} + CO^{DG_i} + NO_x^{DG_i}) * P_{gen}^i + (SO_2^{sub} + CO_2^{sub} + CO^{sub} + NO_x^{sub}) * \left(P_{load}^{part-I} + loss^{part-I} - \sum_{i=1}^{N_{DG}^{part-I}} P_{gen}^i \right) \quad (20)$$

$$Emis^{part-II} = \sum_{i=1}^{N_{DG}^{part-II}} (SO_2^{DG_i} + CO_2^{DG_i} + CO^{DG_i} + NO_x^{DG_i}) * P_{gen}^i$$

$$Emis_{max}^{part-II} = \sum_{i=1}^{N_{DG}^{part-II}} (SO_2^{DG_i} + CO_2^{DG_i} + CO^{DG_i} + NO_x^{DG_i}) * P_{gen}^{max}(i) \quad (21)$$

3 Methodology

Distribution system load flow study is employed for getting the state of network. Proper numbering for each line and bus of the network is required for successfully

Table 3 The values of GA parameters

Parameter	Value
Control variable	$AL_i \in \{1, 2, 3\}$ For load scheduling $P_{gen}^i \in \{1, 2, \dots, N_{DG}^{part-II}\}$ For generation scheduling
Population	80
Cross over probability (P_c)	0.9
Mutation probability (P_m)	0.01
Elitism probability (P_m)	0.05
Maximum iterations	300

implementing any load flow algorithm. If line outage has occurred in a RDS then there is no guarantee that all lines and buses have sequential numbering. Even if they have sequential numbering for a particular slack bus, the sequential number of buses and lines will be modified when slack bus is shuffled between other buses. To avoid these difficulties the following algorithms have been developed.

- Identification of nodes beyond a particular bus
- RDS at single contingency
- Renumbering of buses in part-I of RDS
- Identification of Slack bus and position of each bus from slack bus in part-II of RDS
- Renumbering of buses in part-II of RDS

All these algorithms have been implemented on IEEE 15 bus RDS for enabling legible understanding by considering the outage of the line between buses 2 and 3 in the Appendix of the paper.

3.1 Genetic algorithm and dragonfly algorithm

3.1.1 Genetic algorithm

Genetic algorithm (GA) was first introduced by John Holland and further developed by Goldberg [36]. In GA an array of all control variables is represented by chromosomes and the number of chromosomes generated depends on population size. New generations have been evaluated from old generations using genetic operators like reproduction, cross over and mutation. Elitism operator has been used to keep better individuals of previous generation. The binary-coded genetic algorithm has Hamming cliff problems [37]. Sometimes it creates difficulty for coding of continuous variables and GA requires more computation time and memory. In order to overcome such difficulties, real coded genetic algorithm has been used in this paper. The Step by step procedure for solving a problem using GA is shown in Algorithm 1. The values of GA parameters considered in this paper are as represented in Table 3.

Table 4 The values of DA parameters

Parameter	Value
Control variable	$AL_i \in \{1, 2, 3\}$ For load scheduling
	$P_{gen}^i \in \{1, 2, \dots, N_{DG}^{part-II}\}$ For generation scheduling
Population	80
Weight (w)	0.9–0.4
Separation factor (s)	0.2–0
Alignment factor (a)	0.2–0
Cohesion factor (c)	0.2–0
Food factor (f)	0–2
Enemy factor (e)	0.1–0
Maximum iterations	300

Algorithm 1 Real coded genetic algorithm**Inputs**

- 1: Read number of variables (n)
- 2: Read population size (pop)
- 3: Read cross over probability (P_c)
- 4: Read mutation over probability (P_m)
- 5: Read elitism over probability (P_e)

Steps

- 1: Initialization ▷ Randomly generate a matrix of size popsize rows and n columns, all elements represented in floating values
- 2: Set iter=1
- 3: **while** $iter \leq itermax$ **do**
 - 4: Evaluation ▷ Evaluate objective function for each chromosome
 - 5: Elitism ▷ Selecte most fitted $P_e * pop$ chromosomes
 - 6: Selection ▷ Roulette wheel selection [38]
 - 7: Crossover ▷ Using probability distribution $P(\beta)$ [38]
 - 8: Mutation ▷ Polynomial Mutation [39]
- 9: Replace worst chromosomes of new generation with new chromosomes due to elitism
- 10: iter=iter+1
- 11: **end while**
- 12: Print optimal solution and corresponding objective values

3.1.2 Dragonfly algorithm (DA)

Dragonfly algorithm (DA) was developed by Seyedali Mirjalili [27] based on static (hunting) and dynamic (migration) behavior of Dragonflies. Dragonflies form sub-swarms and fly over different areas in a static swarm for hunting which is the main objective of the exploration phase. In dynamic stage swarm dragonflies form big swarms and fly in one direction for migration which is favorable for exploitation phase. While swarming Dragonflies exhibit some characteristics like separation, alignment,

cohesion, getting attracted towards food source and distracting enemy for survival. Weights corresponding to the above characteristics (s, a, c, f, e) and inertia weight (w) are adaptively tuned for maintaining exploration and exploitation. The step by step procedure for solving a problem using DA is shown in Algorithm 2. The values of DA parameters considered in this paper are as represented in Table 4.

Algorithm 2 Dragonfly Algorithm

Inputs

- 1: Read number of variables (n)
- 2: Read population size (pop)
- 3: Read lower bound (lb) and upper bound (ub) for each variable
- 4: Read maximum step $\Delta x^{max} = \frac{ub-lb}{4}$

Steps

```

1: Initialization      ▷ Randomly generate a position (X) matrix and step (ΔX) matrix between lb and ub
2: Set iter=1
3: while iter ≤ itermax do
4:   Set r =  $\Delta x^{max} + (ub - lb) * \frac{iter}{itermax} * 2$ ;                                ▷ Radius
5:   Set w=0.9-iter* $\frac{0.9-0.4}{itermax}$ ;                                         ▷ Inertia Weight
6:   Set f=2*rand;                                                               ▷ food factor
7:   if iter <  $\frac{itermax}{2}$  then
8:     Set s=2*rand*(0.1-iter* $\frac{0.2}{itermax}$ )                                         ▷ Separation weight
9:     Set a=2*rand*(0.1-iter* $\frac{0.2}{itermax}$ )                                         ▷ Alignment weight
10:    Set c=2*rand*(0.1-iter* $\frac{0.2}{itermax}$ )                                         ▷ Cohesion weight
11:    Set e=(0.1-iter* $\frac{0.2}{itermax}$ )                                              ▷ enemy factor
12:   else
13:     set s=a=c=e=0
14:   end if
15:   Evaluation                                         ▷ Evaluate objective function for each individual
16:   Update food fitness, food position ( $X^+$ ), enemy fitness and enemy position ( $X^-$ ) among all individuals in X
17:   Identify number of neighboring individuals ( $N_i$ ) for each individual i ▷ If distance between  $X_i$  and  $X_j$  is less than 'r' then individuals i and j are neighbors
18:   Compute separation ( $S_i$ ), alignment ( $A_i$ ) and cohesion ( $C_i$ ) for each individual i using Eqs. (22), (23), and (24) if neighbors exist else set all these values to zero

```

$$S_i = - \sum_{j=1}^{N_i} (X_i - X_j) \quad (22)$$

$$A_i = \frac{\sum_{j=1}^{N_i} \Delta X_j}{N_i} \quad (23)$$

$$C_i = \frac{\sum_{j=1}^{N_i} X_j}{N_i} - X_i \quad (24)$$

19: Compute distance (D_{fi}) between X_i and X^+ and distance (D_{ei}) between X_i and X^- for each individual 'i' ▷ j belongs to set of neighboring individuals of i

20: **if** all ($D_{fi} \leq r$) **then** ▷ Checking whether individual 'i' is neighbor for X^+ or not

21: Set $F_i = X^+ - X_i$

22: **else**

23: Set $F_i = 0$

```

24: end if
25: if all  $(D_{ei}) \leq r$  then           ▷ Checking whether individual 'i' is neighbor for  $X^-$  or not
26:    $E_i = X^- + X_i$ 
27: else
28:   Set  $E_i = 0$ 
29: end if
30: if any  $(D_{fi}) > r$  then           ▷ Checking whether individual 'i' is neighbor for  $X^+$  or not
31:   if  $N_i > 1$  then                 ▷ Checking whether individual 'i' has neighbors or not
32:     Set  $\Delta X_i = w * \Delta X_i + rand * A(i) + rand * C(i) + rand * S(i)$  ▷ Updating step vector
       $(\Delta X_i)$  of individual i
33:     Set  $X(i)=X(i)+\Delta X_i$            ▷ Updating position vector ( $X_i$ ) of individual i
34:   else
35:      $X(i)=X(i)+Levy(d)*X(i);$       ▷ Updating position vector ( $X_i$ ) of individual i
36:     Set  $\Delta X_i=0$                   ▷ Updating step vector ( $\Delta X_i$ ) of individual i
37:   end if
38: else
39:   Set  $\Delta X_i=(a*A(i)+c*C(i)+s*S(i)+f*F(i)+e*Enemy(i)) + w*\Delta X_i$  ▷ Updating step vector ( $\Delta X_i$ )
      of individual i
40:    $X(i)=X(i)+\Delta X_i;$            ▷ Updating position vector ( $X_i$ ) of individual i
41: end if
42: end while
43: Print optimal solution and corresponding objective values

```

3.2 Hybrid genetic dragonfly algorithm (HGDA)

In order to achieve a global optimal solution by any population based algorithm, proper balancing is required between exploration and exploitation of the search space. Exploration related to global search in search space and exploitation related to local search in search space are based on current best solution. Too much of diversification and intensification will result in increasing convergence time and increasing the possibility of the solution getting trapped into local optimum point [40].

Genetic Algorithm has a problem in finding the exact solution but it is good at reaching towards global region and slow convergence. GA works based on evolution from generation to generation by not considering individual in the same generation. Basic GA has no memory which means previous knowledge of the problem stands destroyed once the population changes [41]. But this problem can be overcome by including elitism concept. This means that GA with elitism concept has memory which stores best individual from previous population.

However in contrast with GA, DA has fast convergence and its performance is increased as best individuals are available but it does not have internal memory. Due to absence of internal memory DA never maintains tracking on possible set of solutions which have the potential to converge to global optimum that may result in trapping the solution towards local optimum point [42].

To overcome the above drawbacks a novel hybrid algorithm based on GA and DA has been proposed in this paper to exploit the advantages of both GA and DA algorithms. This hybridization includes two additional features to DA like internal memory and improvise searching capability. The proposed hybrid genetic dragonfly algorithm acquires good local and global searching capability to avoid the problem

of trapping the solution towards local optimum point. The step by step procedure for HGDA is shown in Algorithm 3.

Algorithm 3 Hybrid Genetic Dragonfly Algorithm (HGDA)

Inputs

- 1: Read number of variables (n)
- 2: Read population size (pop)
- 3: Read cross over probability (P_c)
- 4: Read mutation over probability (P_m)
- 5: Read elitism over probability (P_e)
- 6: Read lower bound (lb) and upper bound (ub) for each variable
- 7: Read maximum step Δx^{max}

Steps

- 1: Initialize X ▷ Randomly initialize population
- 2: Initialize ΔX ▷ Randomly initialize step vector of size $\frac{pop}{2}$ rows and n columns
- 3: Set iter=1
- 4: **while** $iter \leq itermax$ **do**
- 5: Evaluation ▷ Evaluate objective function for each individual of X
- 6: Sort population (X) based on objective function value and choose top half population (X_{half}) ▷ Sort either in ascending order for minimization problem or in descending order for maximization problem
- 7: Implement steps 5, 6, 7, 8 and 9 of Algorithm 1 on X_{half} population and generate new population X_{GA}
- 8: Implement steps 4 to 41 of Algorithm 2 on X_{half} population and generate new population X_{DA}
- 9: Form new population X consisting of pop individuals by vertically concatenating X_{GA} and X_{DA}
- 10: **end while**
- 11: Print optimal solution and corresponding objective values

3.3 Computation of LMP using hybrid genetic dragonfly algorithm based optimal power flow (HGDA-OPF)

The hybrid genetic dragonfly algorithm based optimal power flow for computing LMP value for each DG unit for load scheduling by employing Algorithm 4 and for generation scheduling by employing Algorithm 5 respectively. Complete flowchart for computing LMP using HGDA-OPF is presented in Appendix.

Algorithm 4 LMP computation using HGDA-OPF for load scheduling

Inputs

- 1: Read linedata of RDS
- 2: Read DG units size ($P_{gen}^{max}(i)$), power factor and location
- 3: Read outage line ($Line_{out}$)
- 4: Read cross over probability (P_c)
- 5: Read mutation over probability (P_m)
- 6: Read elitism over probability (P_e)
- 7: Read population size (pop)
- 8: Read maximum step Δx^{max}

Steps

- 1: Set $P_{gen}^i = P_{gen}^{max}(i)$ for $i=1,2,\dots,N_{DG}^{part-II}$
- 2: Split the network data based on $Line_{out}$ and renumber buses using flowcharts in Figs. 11, 12, 14 and 15
- 3: Set number of control variables $ncv=N_{type}^{part-II}$ ▷ Control variables are AL_i for $i \in 1,2,3$
- 4: Update AL_i^{UL} and TL_i using Eq. (5) or Eq. (6)
- 5: Update P_{Load}^{Mod} of part-II of network using Eq. (8) or Eq. (9).
- 6: Initialize X of size [pop,n] ▷ Randomly initialize AL_i for $i \in 1,2,3$ between AL_i^{LL} and AL_i^{UL}
- 7: Initialize step vector ΔX of size $[\frac{pop}{2}, n]$ ▷ Randomly initialize AL_i for $i \in 1,2,3$ between AL_i^{LL} and AL_i^{UL}
- 8: Set iter=1
- 9: **while** $iter \leq itermax$ **do**
- 10: Update load data of part-II of network for each individual in X as shown in Eqs. (11), (12), (13), (14), and (15).
- 11: Evaluation ▷ Evaluate objective function for each individual of X
- 12: Apply steps 6, 7, 8 and 9 in Algorithm 3. Use step 10 of this Algorithm 4 as and when required.
- 13: **end while**
- 14: Compute LMP value for each DG using Eq. (16)
- 15: Print optimal solution and corresponding objective values

Algorithm 5 LMP computation using HGDA-OPF for generation scheduling

Inputs

- 1: Read linedata of RDS
- 2: Read DG units size ($P_{gen}^{max}(i)$), power factor and location
- 3: Read outage line ($Line_{out}$)
- 4: Read cross over probability (P_c)
- 5: Read mutation over probability (P_m)
- 6: Read elitism over probability (P_e)
- 7: Read population size (pop)
- 8: Read maximum step Δx^{max}

Steps

- 1: Split the network data based on $Line_{out}$ and renumber buses using flowcharts in Figs. 11 and 12
- 2: Set number of control variables $ncv=N_{DG}^{part-II}$ ▷ Control variables are P_{gen}^i for $i \in 1,2,\dots,N_{DG}^{part-II}$
- 3: Update $P_{gen}^{LL}(i)$ and $P_{gen}^{UL}(i)$ as shown in Table 2
- 4: Initialize X of size [pop,ncv] ▷ Randomly initialize P_{gen}^i for $i \in 1,2,\dots,N_{DG}^{part-II}$ between $P_{gen}^{LL}(i)$ and $P_{gen}^{UL}(i)$

5: Initialize step vector ΔX of size $[\frac{pop}{2}, ncv]$ \triangleright Randomly initialize P_{gen}^i for $i \in 1, 2, \dots, N_{DG}^{part-II}$ between $P_{gen}^{LL}(i)$ and $P_{gen}^{UL}(i)$
 6: Set iter=1
 7: **while** $iter \leq itermax$ **do**
 8: Provide renumbering to each line and bus in part-II of network using flowcharts in Figs. 14 and 15 for each individual in X (if required)
 9: Evaluation \triangleright Evaluate objective function shown in Eq. (19) based on constraints shown in Eq. (20) for each individual of X
 10: Apply steps 6, 7, 8 and 9 in Algorithm 3. Use step 8 of this Algorithm 5 as and when required.
 11: **end while**
 12: Compute LMP value for each DG using Eq. (16)
 13: Print optimal solution and corresponding objective values

4 Analytical studies

4.1 Case study-1

The proposed HGDA based OPF has been implemented on 38 bus RDS to compute LMP values at DG buses in part-II of network under MATLAB [43] environment. The system data for 38 bus RDS was taken from [44]. Location and type of each DG unit of capacity 50MW operating at 0.9 lagging power factor are shown in Table 5. Cost function coefficients of each type of DG unit is considered from the paper in [13]. The duration of each line l outage OT_l is assumed as 1 hour, and the market price for active power generation is assumed as 32.38 \$/MWh.

4.1.1 Load scheduling

The line between buses 5 and 6 was considered as an outage line. As the total load is more than the available generation in part-II of network, LMP values of each DG unit in part-II of network is computed by scheduling the load. The Proposed HGDA based OPF has been implemented 10 times on part-II of 38 bus RDS. Out of 10 runs the best objective function (EENS) value is considered for estimating the state of part-II of RDS. Best, worst and average objective function values are shown in Table 6 for $\omega_1=0.333$, $\omega_2=0.333$ and $\omega_3=0.333$.

Table 5 Type and location of DG units in 38 bus RDS

DG unit	Type	Location	Engine type
DG1	1	5	Combined cycle gas turbines
DG2	1	11	Combined cycle gas turbines
DG3	2	19	Gas internal combustion engines
DG4	3	23	Diesel internal combustion engines
DG5	3	27	Diesel internal combustion engines
DG6	2	29	Gas internal combustion engines

Table 6 HGDA-OPF performance in terms of EENS (MWh)

	Best	Average	Worst
	56.4	56.6	57.1

Table 7 DG units generation (MW) and LMP (\$/MWh) for 38 bus RDS

Unit	DG1	DG2	DG3	DG4	DG5	DG6
LMP	32.38	601	32.38	32.38	520	550
Generation	0.98	50	1.17	1.24	50	50

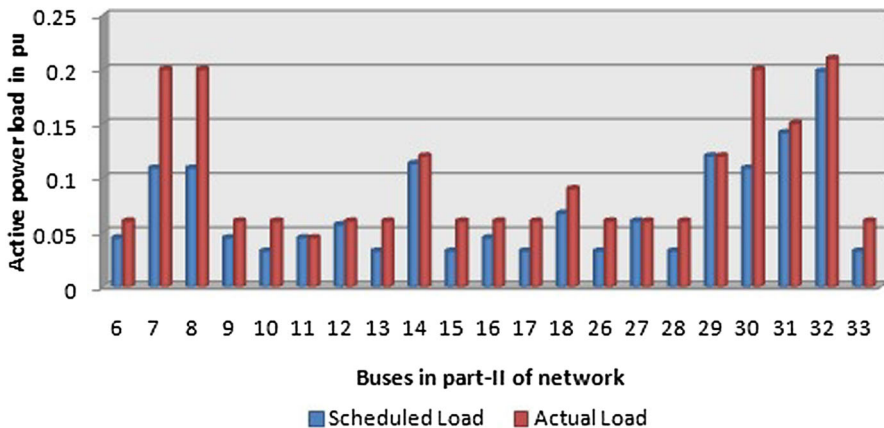


Fig. 1 Scheduled load at each bus in part-II of 38 bus RDS after the line outage between buses 5 and 6

Table 7 presents active power generation and LMP of each DG unit in 38 bus RDS for $\omega_1 = 0.333$, $\omega_2 = 0.333$ and $\omega_3 = 0.333$. As the total generation in part-II of network is 150MW which is less than total load 205.5MW, all DG units in part-II of network can dispatch a maximum capacity of 50MW. The corresponding LMPs are 601 \$/MWh, 520 \$/MWh and 550 \$/MWh. However DG units in part-I of network do not have any contribution in reliability improvement and so no incentive has been provided over and above the market price of 32.38 \$/MWh. DG units in part-I of network generate power as represented in Table 7 such that DG owners get maximum profit for given LMP.

Figure 1 shows the scheduled load at each bus in part-II of network using proposed HGDA based OPF method while considering equal priority among all type of loads. There is no load curtailment at buses 11, 27 and 29 as DG units which were installed at these buses supply total load. Total curtailed load on part-II of network is 56.4 MW. As repair time is considered as 1 hour, EENS value is 56.4 MWh.

Figure 2 shows the actual voltage (V_{act}) at each bus in part-II of network at $\omega_1 = 0.333$, $\omega_2 = 0.333$ and $\omega_3 = 0.333$. All bus voltages are within maximum limit (V_{max}) 1.02 pu and minimum limit (V_{min}) 0.9 pu. It means that the proposed HGDA based OPF method will schedule the loads such that all voltages are within the limits.

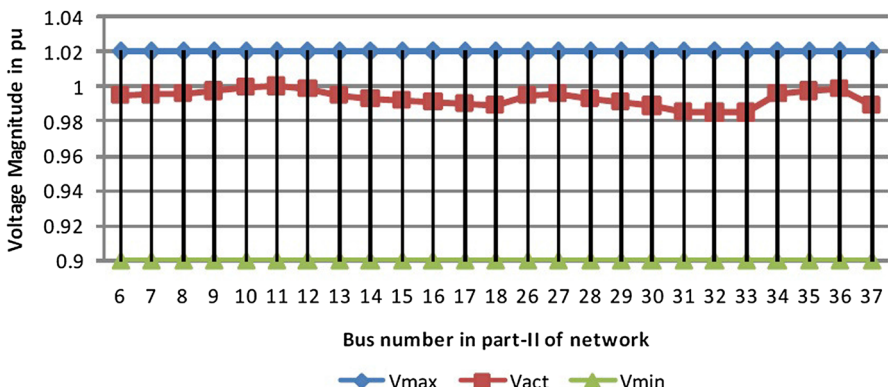


Fig. 2 Voltage at each bus in part-II of 38 bus RDS after the line outage between buses 5 and 6

Table 8 Impact of ω_1 , ω_2 and ω_3 on EENS in 38 bus RDS

ω_1	ω_2	ω_3	$EENS_1(MWh)$	$EENS_2(MWh)$	$EENS_3(MWh)$	EENS(MWh)
0.6	0.3	0.1	10.3	30.8	15.5	56.6
0.3	0.6	0.1	17.4	14.4	25.2	57.0
0.1	0.6	0.3	26.6	26.5	3.5	56.6
0.1	0.3	0.6	24.7	31.7	0.00	56.5
0.6	0.1	0.3	0.00	50.8	5.6	56.4

The impact of weights corresponding to residential, commercial and industrial loads on EENS is shown in Table 8. As weight ω_1 corresponding to residential load increases, EENS value corresponding to residential load decreases. Similarly as ω_2 and ω_3 increases EENS value corresponding to commercial and industrial loads decreases respectively. EENS value for overall system remains almost constant as the generation does not change. However small changes in EENS value for the overall system are due to variations in loss.

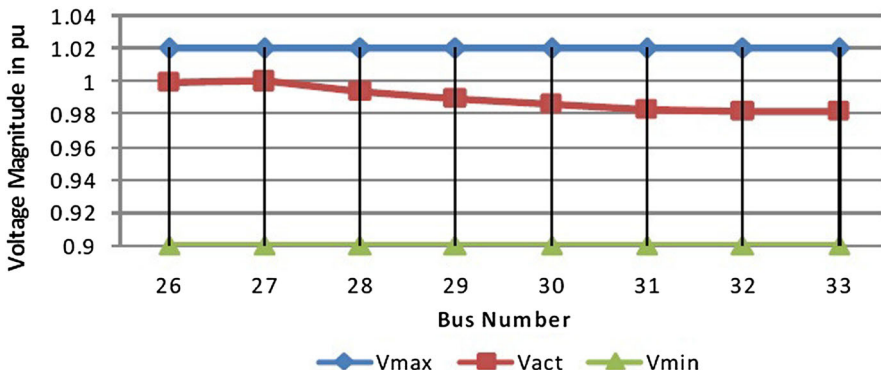
4.1.2 Generation scheduling

Consider the line between buses 6 and 26 as an outage line. The proposed HGDA based OPF computes LMP and generation of each DG unit in part-II of network using generation scheduling as the total load of 0.92 pu is less than the generated power of 1.0 pu in part-II of network. The computed values of LMP and the generation of each DG unit by the proposed method is presented in Table 9 after assigning same weights to all objectives. As there is no contribution from DG units in part-I of network, no incentive has been provided over and above the market price.

Generation of each DG unit in part-II of network has been scheduled using the proposed HGDA based OPF method so that voltage at each bus in part-II of network must be between V_{max} and V_{min} . Computed voltage (V_{act}) at each bus in part-II of network for equal weights among the objectives is shown in Fig. 3.

Table 9 DG units generation (MW) and LMP (\$/MWh) in 38 bus RDS

Unit	DG1	DG2	DG3	DG4	DG5	DG6
LMP	32.38	32.38	32.38	32.38	457.5	543.1
Generation	0.98	0.98	1.17	1.24	43.75	49.35

**Fig. 3** Voltage at each bus in part-II of 38 bus RDS after the line outage between buses 6 and 26**Table 10** Impact of ω_{inv} , ω_{emis} and ω_{los} in 38 bus RDS

ω_{inv}	ω_{emis}	ω_{los}	$DISCO_{inv}^{part-II}$ (\$)	$Emis^{part-II}$ (kg)	$Loss^{part-II}$ (kW)
0.6	0.3	0.1	46735	51019	1115.7
0.3	0.3	0.3	46824	50922	1106.7
0.3	0.6	0.1	46856	50890	1103.734
0	0	1	46857	50891	1103.73

Table 10 shows the impact of ω_{inv} , ω_{emis} and ω_{los} values on DISCO's investment in purchasing power from DG owners, the emission released from part-II of network and the loss in part-II of network respectively. DISCO's decision maker can increase the ω_{inv} to supply total load by purchasing more power from low cost coefficients generator. As the value of ω_{inv} increases, DISCO's investment in purchasing power from DG owners decreases.

Similarly DISCO's decision maker can supply a total load at less emission by increasing ω_{emis} . As the value of ω_{emis} is increases, DISCO gets power from low emission coefficient generators which leads to reduction in emission. It can be inferred from Table 10 that the weights combination of [0,0,1] has reduced emissions in comparison with the weights combinations of [0.6 0.3 0.1] and [0.3 0.3 0.3] despite the value of ω_{emis} is reduced to zero. It is due to the huge positive impact of DG6 on loss reduction. Further it can be inferred from the Table 10 that the weights combination of [0.6 0.3 0.3] has increased emissions in comparison with weights combination of [0.3

Table 11 Impact of ω_{inv} , ω_{emis} and ω_{los} on generation and LMP in 38 bus RDS

ω_{inv}	ω_{emis}	ω_{los}	Generation (kW)		LMP (\$/MWh)	
			DG5	DG6	DG5	DG6
0.6	0.3	0.1	44380	48740	463.777	536.618
0.3	0.3	0.3	43754	49352	457.541	543.136
0.3	0.6	0.1	43551.6	49551.6	455.516	545.247
0	0	1	43552.1	49552.1	455.521	545.252

0.3 0.3] despite the value of ω_{emis} remains same. It is due to the influence of low cost and high emission generator DG5 over high cost and low emission generator DG6.

DISCO can reduce active power loss of network by increasing ω_{los} . Active power loss in part-II of network having the weights combination of [0.6 0.3 0.1] is more in comparison with weights combination of [0.3 0.6 0.1] despite the value of ω_{los} is the same in both cases. It is due to high positive impact of low emission coefficients generator (DG6) on active power loss reduction. Active power loss of network is less having the weights combination of [0.3 0.6 0.1] in comparison with weights combination of [0.3 0.3 0.3] despite the weight corresponding to ω_{los} is increased. It is due to increasing priority for DG6 generation that has a huge positive impact on loss reduction.

Table 11 presents the impact of ω_{inv} , ω_{emis} and ω_{los} on active power generation and LMP values of DG units in part-II of network. As ω_{inv} increases, DISCO's decision maker is willing to get power from low fuel cost coefficients generator which leads to an increase in the generation and LMP value of DG5 (low fuel cost coefficients generator). However with the weights combination of [0,0,1] the generation and LMP of DG5 are more in comparison with the weights combination of [0.3 0.6 0.1] despite the value of ω_{inv} is increased. It is also due to contribution of DG5 in active power loss reduction.

Similarly if ω_{emis} increases at lower ω_{los} values then generation and LMP value of DG6 (low emission coefficients generator) increases. However, at $\omega_{los}=1$, high priority is given to loss reduction, generation and LMP value of DG6 are more even when $\omega_{emis}=0$. It is due to the high impact of DG6 on loss reduction. With the weights combination of [0 0 1] active power generation of DG6 is more than DG5. It is due to the positive impact of DG6 on active power loss reduction which is more than DG5.

State of part-I of network has been observed in terms of active power loss and voltage magnitude. No DG units in part-I of network have any impact on reliability improvement. DISCO does not provide any incentives over the market price to these units. Hence LMP value for each DG unit in part-I of network is equal to market price i.e 32.38 (\$/MWh). DG units in part-I of network will dispatch generation such that the DG owner gets maximum profit at a given LMP. Voltage at each bus in part-I of network while considering line outage between 5 and 6 are shown in Fig. 4 and the active power loss is 1.78MW. Similarly Fig. 5 shows voltage at each bus in part-I of network while considering line outage between buses 6 and 26 and the active power

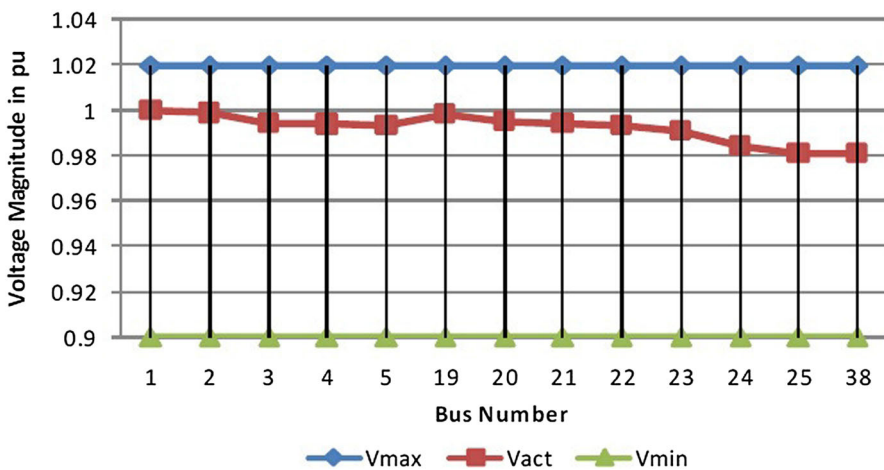


Fig. 4 Voltage at each bus in part-I of 38 bus RDS after line outage between buses 5 and 6

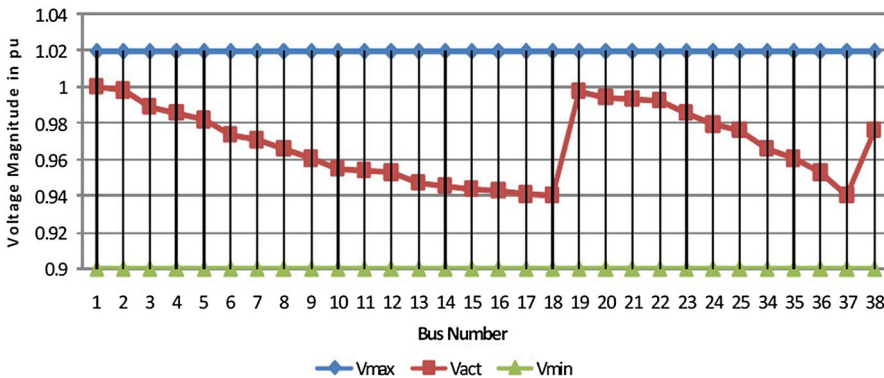


Fig. 5 Voltage at each bus in part-I of 38 bus RDS after line outage between buses 6 and 26

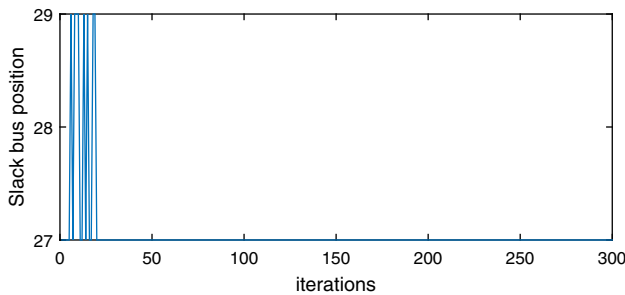


Fig. 6 Shuffling of slack bus position in part-II of 38 bus RDS

loss in part-I of network is 7.05MW. Shuffling of slack bus between buses 27 and 29 in part-II of network is shown in Fig. 6. This shuffling occurred due to change of bus which has maximum injection.

Table 12 LMP values for different line outages in 38 bus RDS

Line	LMP in \$/MWh						HGDA EENS(MWh)	Basecase EENS(MWh)
	DG1	DG2	DG3	DG4	DG5	DG6		
1	601	601	550	520	520	550	73.6	371.5
3	32.38	32.38	32.38	32.38	32.38	32.38	27	27
4	32.38	32.38	32.38	32.38	32.38	32.38	18	18
6	601	601	32.38	520	520	550	76.9	325.5
14	32.38	32.38	32.38	32.38	457.54	543.14	0	92

Table 12 presents LMP value of each DG unit in test system for different line outages and at equal weights among objectives. As there is no DG unit in part-II of network for outage of line 3 or 4, EENS value provided by the proposed method is equal to base case EENS value. As all DG units are located in part-I of network and there is no contribution from these units on reliability improvement, no incentive has been provided over the market price. Hence LMP value of each DG unit for outage of line 3 or 4 is equal to market price of 32.38 \$/MWh. For the outage of remaining lines such as 1, 6 and 14, the EENS value by proposed method is less compared to base case. This is due to the presence of DG units in part-II of network. LMP values shown in Table 12 are based on DG unit's contribution on EENS reduction and fuel cost coefficients. LMP of DG3 for outage of line 6 and, DG1, DG2, DG3 and DG4 for outage of line 14 is equal to the market price of 32.38 \$/MWh as these units are located in part-I of network.

Table 13 presents active power generation of each DG unit for different line outages and at equal priorities among objectives. All DG units in part-I of network due to the outage of any line generate active power such that the owners will receive maximum profit at the market price of 32.38\$/MWh. All DG units in part-II of the network due to outage of either line 1 or 6 dispatch maximum capacity as the total load in part-II of the network is more than available generation. DG units in part-II of network due to outage of line 14 such as DG5 and DG6 generate 43.75 MW and 49.35 MW respectively based on DISCO's priority on DISCO's investment purchase power from DG owners, emission and loss of part-II network. EENS value for each type of customers is the same as base case in case of no DG in part-II of network; otherwise EENS value for each type of customers is less than base case values as DG units supply load in part-II of network.

Table 14 presents DISCO's investment to purchase power from DG owners and grid, emission and active power loss in part-I and part-II of network for different line outages and equal priorities among stated objectives. The values of DISCO's investment, emission and loss in part-I of network are zero as no load exists in part-I of network while considering line 1 as an outage line. Similarly these values are zero in part-II of the network for outage of line 3 or 4 as no DG exists in part-II of network. The values of $DISCO_{inv}^{part-I}$ and $Emis^{part-I}$ are obtained based on the amount of power purchased from grid and DG owners. However the values in part-II of network are based on power purchased from DG owners only.

Table 13 DG units active power generation for different line outages in 38 bus RDS

Line	Generation in MW				HGDA			Base case		
	DG1	DG2	DG3	DG4	DG5	DG6	$ENN S_1$ (MWh)	$ENN S_2$ (MWh)	$ENN S_3$ (MWh)	$ENN S_3$ (MWh)
1	50	50	50	50	50	30.9	42.7	0	88	232.5
3	0.981	0.981	1.17	1.24	1.24	1.17	9	9	9	9
4	0.981	0.981	1.17	1.24	1.24	1.17	9	0	9	0
6	50	50	1.17	50	50	0.886	71.45	4.58	60	223.5
14	0.981	0.981	1.17	1.24	43.75	49.35	0	0	36	42
									50	6

Table 14 DISCO's investment, emission and active power loss for different line outages in 38 bus RDS

Line	Part-I of network		Part-II of network			
	$DISCO_{inv}^{part-I}$ (\$)	$Emissions^{part-I}$ (kg)	$Loss^{part-I}$ (kW)	$DISCO_{inv}^{part-II}$ (\$)	$Emissions^{part-II}$ (kg)	$Loss^{part-II}$ (kW)
1	0	0	0	167100	180396.2	2099.1
3	11154.97	332446.1	17348	0	0	0
4	11446.4	341197.8	17407	0	0	0
6	1489.58	44153.24	127.92	139600	156544.2	1410.8
14	9050.27	270249	7053.2	46824	50922	1106.7

Table 15 Comparison of reliability in 38 bus RDS for line outage between bus 5 and bus 6

EENS in kWh					
	HGDA	GA [38]	DA [27]	Uniform price method [15]	Base case
EENS (kWh)	56399.7	56489.6	56421.3	202110	205500
Time (s)	317	240	150	—	—

Table 16 Comparison of objective function values and EENS in 38 bus RDS for line outage between buses 6 and 26

	HGDA	GA [38]	DA [27]	Uniform price method[15]	Base case
Objective function value	0.75369	0.75493	0.75432	0.00854	0
EENS (kWh)	0	0	0	89590	92000
Time (S)	148	118	99.6	—	—

Table 15 shows comparison of the proposed method with GA, DA and uniform price method in terms of EENS value for outage of line between buses 5 and 6. The proposed method provides least EENS value in comparison with other methods. It can be inferred that the proposed method effectively improves reliability of network by providing proper incentives to DG units in terms of LMP.

Table 16 shows comparison of the proposed method with GA, DA and uniform pricing method by considering line outage between buses 6 and 26. Proposed method, GA and DA provides better results compared to uniform pricing method in terms of EENS value. As all iterative methods have the same EENS value, the effectiveness of the proposed method has been compared with objective function value. The proposed method provides better objective function value compared to GA and DA.

Figure 7 presents the comparison between convergence characteristics of HGDA, DA and GA. GA takes more number of iterations to converge, and as it gives minimum value of objective function at 300th iteration. It can be inferred that there is no guarantee that this solution is close to global solution. DA converges at around 230th iteration. It shows that DA is converging at fewer number of iterations compared to GA. As HGDA is hybridization of GA and DA, the number of iterations taken by HGDA to converge is between GA and DA. As HGDA has good local and global searching capability, it provides better solution close to global as compared to DA and GA.

4.2 Case study-2

The proposed HGDA based OPF has been implemented on Pacific Gas and Electric Company (PG&E) 69 bus RDS to verify the performance. The line data and bus data of PG&E 69 bus RDS as shown in Table 25 is drawn from the paper in [45]. It is assumed that all the DG units have the capacity of 1MW at 0.9 lagging power factor.

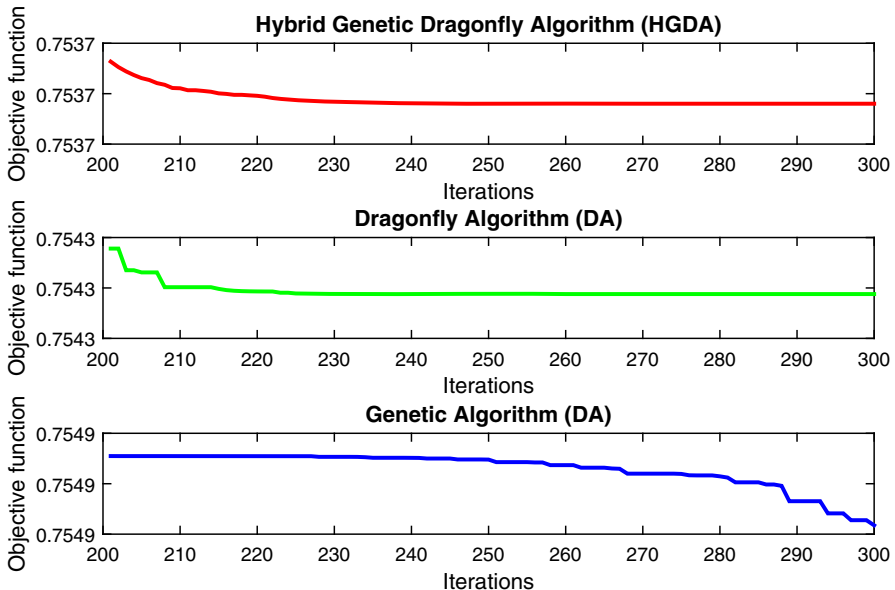


Fig. 7 Convergence characteristics of HGDA, DA and GA in 38 bus RDS

Table 17 Type and Location of DG units in PG & E 69 bus RDS

DG unit	Type	Location	Engine type
DG1	1	61	Combined cycle gas turbines
DG2	2	53	Gas internal combustion engines
DG3	3	11	Diesel internal combustion engines

The location and type of each DG is shown in Table 17. In this study, the market price for active power generation is considered as 21.59 \$/MWh.

4.2.1 Load scheduling

The performance of the proposed method during load scheduling on PG & E 69 bus RDS has been observed by considering the line between buses 3 and 4 as an outage line. The obtained results in terms of EENS, generation and LMP values are presented in Table 18. EENS value for each type of loads is changed based on combination of priorities (in terms of weights ω_1 , ω_2 and ω_3) considered. EENS value of any type of load is reduced to zero by keeping priority 1 (high priority) for that type of load. Small change in overall EENS value at different weight combinations even when generation remains constant is due to variation in active power loss in network. As total load in part-II of network is more than available generation, all three DG units injecting power in to the network up to maximum capacity of 1 MW and corresponding LMP values are 32.6 \$/MWh, 30.6 \$/MWh and 30 \$/MWh respectively. These LMP values have

Table 18 Impact of ω_1 , ω_2 and ω_3 on EENS, DG units generation and LMP in PG&E 69 bus RDS

ω_1	ω_2	ω_3	EENSR	EENSC	EENSI	EENS	Generation in kW			LMP in \$/MWh		
							DG1	DG2	DG3	DG1	DG2	DG3
1	0	0	0	0.09	0.46	0.55	1000	1000	1000	32.6	30.6	30
0.6	0.3	0.1	0	0	0.55	0.55	1000	1000	1000	32.6	30.6	30
0.3	0.1	0.6	0	0.5	0.19	0.69	1000	1000	1000	32.6	30.6	30
0.1	0.3	0.6	0.56	0	0	0.56	1000	1000	1000	32.6	30.6	30
0	0	1	0.4	0.47	0	0.87	1000	1000	1000	32.6	30.6	30
0	1	0	0.02	0	0.53	0.55	1000	1000	1000	32.6	30.6	30

Table 19 DG units generation, LMP and EENS at different line outages in PG&E 69 bus RDS

Line	Generation in kW			LMP in \$/MWh			$EENS_l$ (kW)	$EENS_{base}^l$ (kW)
	DG1	DG2	DG3	DG1	DG2	DG3		
1	1000	1000	1000	32.6	30.6	30	823.06	3802.29
2	1000	1000	1000	32.6	30.6	30	822.71	3802.29
8	1000	884.3	663.1	32.6	29.4	26.6	0	2514.65
52	1000	737.8387	159	32.6	27.82	21.59	0	1717.15

been computed such that DG owners receive maximum profit for generating 1 MW active power.

DG units generation, LMP and EENS for different line outages by considering equal priorities among objectives are presented in Table 19. While considering either line 1 or line 2 as an outage line, all DG units injecting power into the system up to a maximum capacity of 1000 kW have been considered. It was happening due to excess load over the available generation in part-II of network. LMP values for DG1, DG2 and DG3 that correspond to 1000 kW generation are 32.6\$/MWh, 30.6\$/MWh and 30\$/MWh respectively. While considering line 8 as an outage line, DG2 and DG3 generations have been curtailed as available generation is more than load in part-II of network. Similarly while considering line 52 as an outage line, DG2 generation has been curtailed. These generation curtailments are based on priorities considered among DISCO's investment, emission and active power loss. However the DG1 is injecting up to a maximum capacity 1000 kW as local load is more than DG unit capacity. While considering line 52 as an outage line, DG3 is located in part-I of network and it does not have any contribution in reliability improvement. Hence there is no incentive given to DG3 over market price of 21.59\$/MWh. For all tested outages the proposed method improves the reliability of network by decreasing the EENS value.

DISCO's investment to purchase power from grid and DG owners, emission and active power loss for various outages by considering equal priorities among objectives are presented in Table 20. As no load exists in part-I of network, while considering either line 1 or line 2 as an outage line, DISCO's investment to purchase power from grid, emission and active power loss are zero. DISCO's investment and emission

Table 20 DISCO's investment, emission and active power loss at different outages in PG&E 69 bus RDS

Line	Part-I of network			Part-II of network		
	$DISCO_{inv}^{part-I}$ (\$)	$Emis^{part-I}$ (kg)	$Loss^{part-I}$ (kW)	$DISCO_{inv}^{part-II}$ (\$)	$Emis^{part-II}$ (kg)	$Loss^{part-II}$ (kW)
1	0	0	0	93.2	1803.96	21.27
2	0	0	0	93.2	1803.96	20.92
8	54.35	2447.9	2.718	76.2	1517.9	33.18
52	37.47	1632.7	18.46	53.13	1152.6	21.19

in part-I of network are computed based on load at substation bus and DG units generation. However these parameters computed in part-II of network are based on DG units generation only.

4.2.2 Generation scheduling

The performance of the proposed method during generation scheduling has been observed by considering line between buses 4 and 5 as an outage line. Impact of weights ω_{inv} , ω_{emis} and ω_{los} on DG units generation, LMP, DISCO's investment to purchase power from DG owners, emission released from network and network active power loss have been presented in Table 21. As increasing the weight corresponds to emission reduction ω_{emis} , generation and LMP values of the low emission coefficient generator DG2 increases. Which means that low emission coefficient generators receive more incentive from DISCO as and when DISCO increases priority to emission reduction by increasing ω_{emis} . This further results in reduction of network emission. The DG1 is placed at bus 61 where the total load is 1244kW, more than local DG unit (DG1) capacity. Hence DG1 injects the power into the network up to its rated capacity. Hence generation of DG1 at each combination of weights is equal to 1000 kW and the corresponding LMP value is 32.60(\$/MWh).

DG3 is responsible for both loss reduction and DISCO's investment cost reduction due to its low cost coefficients. Hence DG3 generation and LMP, network active power loss and DISCO's investment cost vary based on net weight that corresponds to both loss reduction and investment cost reduction. Net weight (ω_{net}) is equal to sum of weights corresponding to active power loss reduction and DISCO's investment cost reduction. As DG3 generation and LMP values increase, the active power loss of network and DISCO's investment cost decrease with ω_{net} as shown in Table 22.

The proposed method has been compared in terms of objective function value and EENS with some meta heuristic techniques existing in literature, like GA [38], DA [27] and conventional method to compute LMP in RDS such as uniform Price Method [15] in order to demonstrate accuracy and validity. Comparison of the proposed method with other methods have been presented in Table 23. For generation scheduling, uniform price method provides least objective function value but it has more EENS value which is not acceptable from a reliability point of view. However the proposed method provides minimum objective function value compared to GA [38] and DA [27]. The

Table 21 Impact of weights ω_{inv} , ω_{emis} and ω_{los} on DG units generation, LMP, DISCO's investment, emission and loss in PG & E 69 bus RDS

ω_{inv}	ω_{emis}	ω_{los}	Generation (kW)			LMP (\$/MWh)			DISC $C_{inv}^{part-II}$			$E_{emis}^{part-II}$			$Loss^{part-II}$		
			DG1	DG2	DG3	DG1	DG2	DG3	(\$)	(\$)	(\$)	kg	kg	kg	(kW)	(kW)	(kW)
0	1	0	1000	1000	709.5	32.6	30.6	27.1	82.43	1622	1622	33.29	33.29	33.29	33.29	33.29	33.29
0.6	0.3	0.1	1000	918.4	791	32.6	29.74	27.91	81.98	1634	1634	33.11	33.11	33.11	33.11	33.11	33.11
0.3	0.1	0.6	1000	875.9	833.4	32.6	29.28	28.33	81.86	1641	1641	33.06	33.06	33.06	33.06	33.06	33.06
0	0	1	1000	835.3	874.7	32.6	28.85	28.75	81.83	1647	1647	33.04	33.04	33.04	33.04	33.04	33.04
1	0	0	1000	828	881.3	32.6	28.78	28.81	81.82	1648	1648	33.04	33.04	33.04	33.04	33.04	33.04

Table 22 Impact of weights ω_{net} on DG3 generation, LMP, DISCO's investment and loss in PG & E 69 bus RDS

ω_{inv}	ω_{los}	ω_{net}	$DISCO_{inv}^{part-II}$ (\$)	$Loss^{part-II}$ (kW)	Generation (kW)	LMP (\$/MWh)
0	0	0	82.43	33.29	709.5	27.1
0.6	0.1	0.7	81.98	33.11	791	27.91
0.3	0.6	0.9	81.86	33.06	833.4	28.33
0	1	1	81.83	33.04	874.7	28.75
1	0	1	81.82	33.04	881.3	28.81

Table 23 Comparison of proposed HGDA based opf method with other methods on PG&E 69 bus RDS

Scheduling	Parameters	Proposed method	DA[27]	GA [38]	Uniform price method [15]	Base case
Generation	Objective function	0.6450146	0.6450147	0.6451	0.18393	0
	EENS (kW)	0	0	0	2316.95	2676.75
Load	Objective function	0.0818	0.08991	0.11236	0.20232	0.999
	EENS (kW)	550.5	550.8	551.2	3165.2	3525.15

proposed method provides EENS value which is the same as GA [38] and DA [27] for generation scheduling as available generation is more than load in part-II of network. Objective function value in base case is zero as no generation is available in part-II of network. For load scheduling, proposed method provides least EENS value and objective function value in comparison with GA [38], DA [27] and uniform Price Method [15].

5 Conclusion

This paper proposed a hybrid genetic dragonfly algorithm (HGDA) based optimal power flow (OPF) to compute LMP at each DG bus for reliability improvement. This paper enables DISCO to improve system reliability by controlling the private DG owners using financial incentives in terms of LMP. This method has been developed based on consideration that there is no control on DG units located in part-II of network under outage. So this method is developed to specify financial incentives to encourage private DG owners in part-II of network to operate in such a way that reliability is improved. This method can estimate LMP values at any hour of the day and at any line outage. It has been formulated by incorporating voltage limits, line flow limits, generation and load limits. The results show that the DG units which have impact on reliability improvement receive better incentives than the market price. This method also provides information on emission, loss and DISCO's investment to purchase

power from grid and DG owners. This method can estimate state of part-I of network in terms of voltage magnitude and active power loss.

In this paper, the hybridization of the GA and DA for improved results has been implemented for the first time. This process extracts the advantages of both methods and provides better results in comparison with individual method. The computation of LMP at DG buses for improving the reliability of the system has been considered for the first time in this paper.

As integration of DG units in distribution network is bound to increase in future, this work can contribute significantly to the problems related to planning and operation of RDS.

Appendix

38 bus RDS

The single line diagram of 38 bus RDS as shown in Fig. 8 is drawn from [44] and line data and bus data is represented in Table 24.

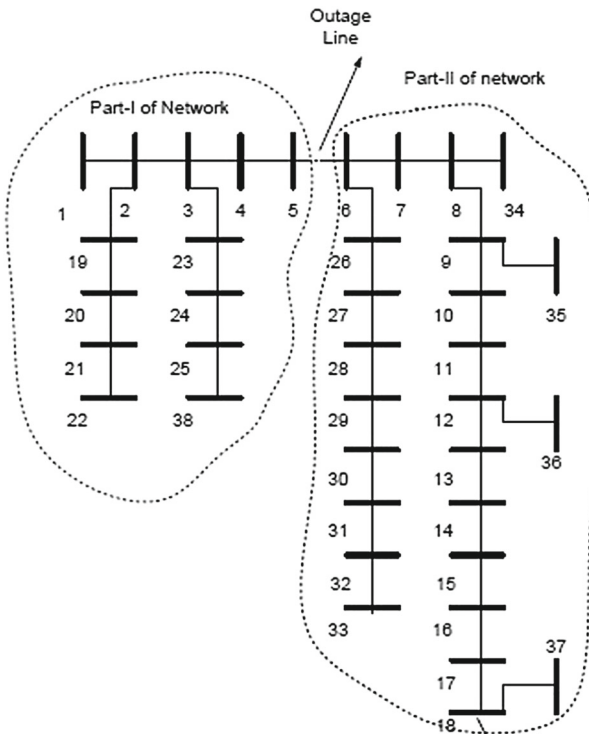


Fig. 8 Single line diagram of 38 bus RDS [44]

Table 24 38 bus RDS data [44]

Line	From	To	P (pu)	Q (pu)	R (pu)	X (pu)	S_f (pu)	Load	Line	From	To	P (pu)	Q (pu)	R (pu)	X (pu)	S_f (pu)	Load
1	1	2	0.1	0.06	0.000574	0.0000293	4.6	1	21	32	33	0.06	0.04	0.002123	0.003301	0.1	2
2	2	19	0.09	0.04	0.001021	0.000974	0.5	1	22	6	7	0.2	0.1	0.001166	0.003853	1.5	2
3	19	20	0.09	0.04	0.009366	0.00844	0.5	2	23	7	8	0.2	0.1	0.00443	0.001464	1.05	2
4	20	21	0.09	0.04	0.00255	0.002979	0.21	3	24	8	34	0	0	0.012453	0.012453	0.5	0
5	21	22	0.09	0.04	0.004414	0.005836	0.11	1	25	8	9	0.06	0.02	0.006413	0.004608	1.05	3
6	2	3	0.09	0.04	0.00307	0.001564	4.1	3	26	9	35	0	0	0.012453	0.012453	0.5	0
7	3	23	0.09	0.05	0.002809	0.00192	1.05	2	27	9	10	0.06	0.02	0.006501	0.004608	1.05	2
8	23	24	0.42	0.2	0.005592	0.004415	1.05	2	28	10	11	0.045	0.03	0.001224	0.000405	1.05	2
9	24	25	0.42	0.2	0.005579	0.004366	0.5	2	29	11	12	0.06	0.035	0.002331	0.000771	1.05	1
10	25	38	0	0	0.003113	0.003113	0.1	0	30	12	36	0	0	0.012453	0.012453	0.5	0
11	3	4	0.12	0.08	0.002279	0.001161	2.9	2	31	12	13	0.06	0.035	0.009141	0.007192	0.5	2
12	4	5	0.06	0.03	0.002373	0.001209	2.9	1	32	13	14	0.12	0.08	0.003372	0.004439	0.45	1
13	5	6	0.06	0.02	0.0051	0.004402	2.9	3	33	14	15	0.06	0.01	0.00368	0.003275	0.3	2
14	6	26	0.06	0.025	0.001264	0.000644	1.5	2	34	15	16	0.06	0.02	0.004647	0.003394	0.25	3
15	26	27	0.06	0.025	0.00177	0.000901	1.5	3	35	16	17	0.06	0.02	0.008026	0.010716	0.25	2
16	27	28	0.06	0.02	0.006594	0.005814	1.5	2	36	17	18	0.09	0.04	0.004558	0.005574	0.1	3
17	28	29	0.12	0.07	0.005007	0.004362	1.5	2	37	18	37	0	0	0.003113	0.003113	0.5	0
18	29	30	0.2	0.6	0.00316	0.00161	1.5	2									
19	30	31	0.15	0.07	0.006067	0.005996	0.5	1									
20	31	32	0.21	0.1	0.001933	0.002253	0.5	1									
Base MVA=100 Base kV=23 Total Active Power load= 371.5MW Total Reactive Power load= 230MVar																	
Type=1: Residential Load & Type 2: Commercial Load																	
Type=3: Industrial Load & Type 0: No Load																	

PG & E 69 bus RDS

The single line diagram of PG & E 69 bus RDS as shown in Fig. 9 is drawn from [45] and line data and bus data is represented in Table 25.

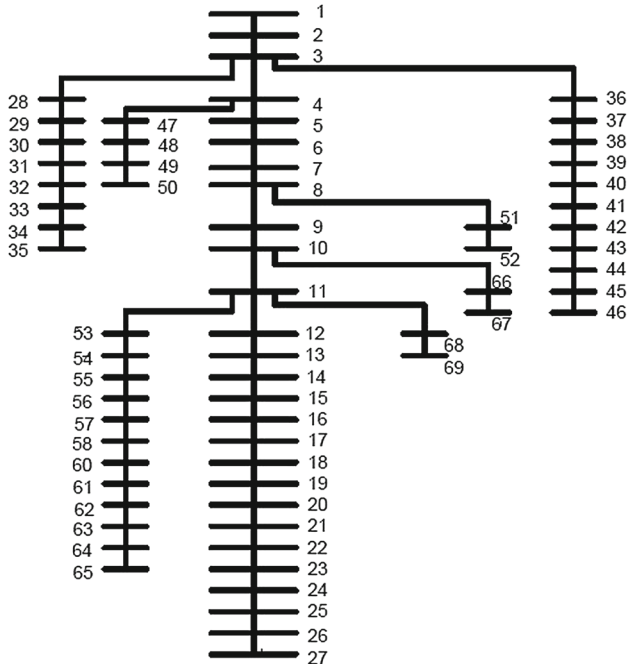


Fig. 9 Single line diagram of PG&E 69 bus RDS [45]

Table 25 PG&E 69 bus RDS data[45]

Line	From	To	P (kW)	Q (kVar)	R (Ohms)	X (Ohms)	S_l (kVA)	Type	Line	From	P (kW)	Q (kVar)	R (Ohms)	X (Ohms)	S_l (kVA)	Type	
1	1	2	0	0	0.0005	0.0012	5858.279	0	35	3	36	26	18.55	0.0044	0.0108	271.4951	1
2	2	3	0	0	0.0005	0.0012	5858.084	0	36	36	37	26	18.55	0.0640	0.1565	233.1679	1
3	3	4	0	0	0.0015	0.0036	5451.529	0	37	37	38	0	0	0.1053	0.1230	194.8057	0
4	4	5	0	0	0.0251	0.0294	4194.268	0	38	38	39	24	17	0.0304	0.0355	194.7749	1
5	5	6	2.6	2.2	0.3660	0.1864	4190.853	1	39	39	40	24	17	0.0018	0.0021	159.4477	1
6	6	7	40.4	30	0.3811	0.1941	4149.53	1	40	40	41	1.2	1	0.7283	0.8509	124.1901	1
7	7	8	75	54	0.0922	0.0470	4050.542	1	41	41	42	0	0	0.3100	0.3623	122.2385	0
8	8	9	30	22	0.0493	0.0251	3866.126	1	42	42	43	6	4.3	0.0410	0.0478	122.2027	1
9	9	10	28	19	0.8190	0.2707	1131.275	1	43	43	44	0	0	0.0092	0.0116	113.3439	0
10	10	11	145	104	0.1872	0.0619	1084.966	2	44	44	45	39.22	26.3	0.1089	0.1373	113.3429	1
11	11	12	145	104	0.7114	0.2351	816.855	2	45	45	46	39.22	26.3	0.0009	0.0012	56.66589	1
12	12	13	8	5	1.0300	0.3400	518.1711	1	46	4	47	0	0	0.0034	0.0084	1256.972	0
13	13	14	8	5.5	1.0440	0.3450	505.3151	1	47	47	48	79	56.4	0.0851	0.2083	1256.909	1
14	14	15	0	0	1.0580	0.3496	492.1793	0	48	48	49	384.7	274.5	0.2898	0.7091	1138.865	3
15	15	16	45.5	30	0.1966	0.0650	490.7164	1	49	49	50	384.7	274.5	0.0822	0.2011	567.3941	3
16	16	17	60	35	0.3744	0.1238	425.1911	1	50	8	51	40.5	28.3	0.0928	0.0473	64.59976	1
17	17	18	60	35	0.0047	0.0016	341.7906	1	51	51	52	3.6	2.7	0.3319	0.1114	5.392506	1
18	18	19	0	0	0.3276	0.1083	258.8745	0	52	9	53	4.35	3.5	0.1740	0.0886	2685.854	1
19	19	20	1	0.6	0.2106	0.0690	258.7494	1	53	53	54	26.4	19	0.2030	0.1034	2671.587	1
20	20	21	114	81	0.3446	0.1129	257.2771	2	54	54	55	24.4	17.2	0.2842	0.1447	2623.822	1
21	21	22	5	3.5	0.0140	0.0046	89.72512	1	55	55	56	0	0	0.2813	0.1433	2576.099	0
22	22	23	0	0	0.1591	0.0526	82.41798	0	56	56	57	0	0	1.5900	0.5337	2564.558	0
23	23	24	28	20	0.3463	0.1145	82.4118	1	57	57	58	0	0	0.7837	0.2630	2505.189	0

Table 25 continued

Line	From	To	P (kW)	Q (kVar)	R (Ohms)	X (Ohms)	S_l (kVA)	Type	Line	From	To	P (kW)	Q (kVar)	R (Ohms)	X (Ohms)	S_l (kVA)	Type
24	24	25	0	0	0.7488	0.2475	41.20428	0	58	59	100	72	0.3042	0.1006	2475.973	2	
25	25	26	14	10	0.3989	0.1021	41.19702	1	59	59	60	0	0.3861	0.1172	2317.734	0	
26	26	27	14	10	0.1732	0.0572	20.59721	1	60	60	61	1244	888	0.5075	0.2585	2305.252	3
27	3	28	26	18.6	0.0044	0.0108	134.8741	1	61	61	62	32	23	0.0974	0.0496	466.4746	1
28	28	29	26	18.6	0.0040	0.1565	96.51161	1	62	62	63	0	0	0.1450	0.0738	419.3933	0
29	29	30	0	0	0.3978	0.1315	58.1433	0	63	63	64	227	162	0.7105	0.3619	419.2166	3
30	30	31	0	0	0.0702	0.0232	58.13626	0	64	64	65	59	42	1.0410	0.5302	86.28402	1
31	31	32	0	0	0.3510	0.1160	58.13501	0	65	11	66	18	13	0.2012	0.0611	53.20166	1
32	32	33	14	10	0.8390	0.2816	58.1288	1	66	66	67	18	13	0.0047	0.0014	26.59929	1
33	33	34	19.5	14	1.7080	0.5646	37.4686	1	67	12	68	28	20	0.7394	0.2444	82.45926	1
34	34	35	6	4	1.4740	0.4873	8.653876	1	68	68	69	28	20	0.0047	0.0016	41.21563	1
Base MVA=10 Base kV=12.66 Total Active Power load= 3802.3kW Total Reactive Power load= 2694.1kVar																	
Type=0: No Load & Type=1: Residential Load & Type 2: Commercial Load & Type=3: Industrial Load																	

Prerequisite algorithms

The single line diagram of IEEE 15 bus RDS is shown in Fig. 10 and the line data and bus data are represented in Table 26.

Fig. 10 IEEE 15 Bus RDS [46]

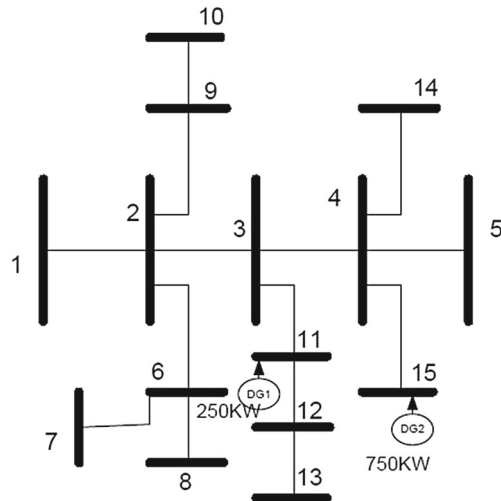


Table 26 IEEE 15 bus RDS data [46]

Line	From	To	P (pu)	Q (pu)	R (pu)	X (pu)
1	1	2	0.2205	0.2249	0.002237	0.002188
2	2	3	0.35	0.357	0.001934	0.001892
3	3	4	0.7	0.7141	0.00139	0.00136
4	4	5	0.2205	0.2249	0.002518	0.001699
5	2	9	0.35	0.357	0.003328	0.002244
6	9	10	0.2205	0.2249	0.002788	0.00188
7	2	6	0.7	0.7141	0.004227	0.002851
8	6	7	0.7	0.7141	0.001799	0.001213
9	6	8	0.35	0.357	0.002068	0.001395
10	3	11	0.7	0.7141	0.002968	0.002002
11	11	12	0.35	0.357	0.004047	0.00273
12	12	13	0.2205	0.2249	0.003328	0.002244
13	4	14	0.35	0.357	0.003687	0.002487
14	4	15	0.7	0.7141	0.001979	0.001335

Base KVA=200 Power factor of load =0.7 Base kV=11

Active power load = 1.2264MW Reactive power load = 1.2510MVar

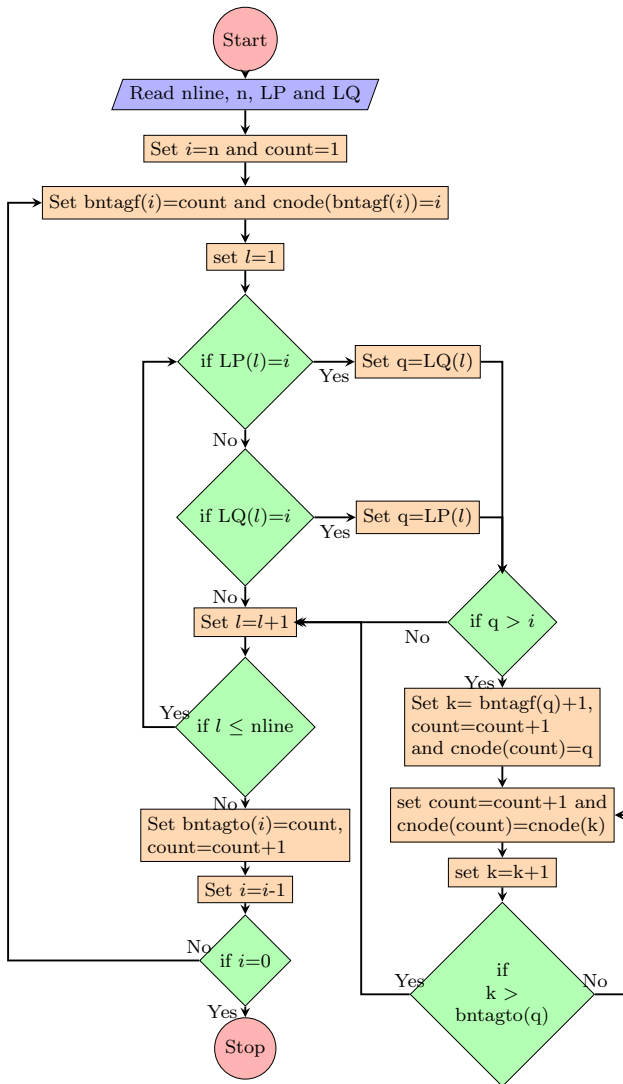


Fig. 11 Flowchart to identify nodes beyond a particular bus

Identification of nodes beyond a particular bus

The process of identifying nodes connected beyond a particular bus is presented in the flowchart as shown in Fig. 11. The proposed algorithm can be helpful to distribution network decision maker to get information about nodes which are disconnected from substation bus due to outage. This method can also be helpful to implement some of the load flow methods in RDS where information of nodes connected beyond a particular node is required as in [46, 47].

Table 27 bntagf and bntagto matrices of IEEE 15 bus RDS

Bus	1	2	3	4	5	6	7	8	9	10	11	12	13	14	15
bntagf	44	30	22	18	17	14	13	12	10	9	6	4	3	2	1
bntagto	58	43	29	21	17	16	13	12	11	9	8	5	3	2	1

Table 28 Information of cnode vector of IEEE 15 bus RDS

Bus	15	14	13	12	11			10	9	8	7	6			
cnode	15	14	13	12	13	11	12	13	10	9	10	8	7	6	7
Bus	6	5	4				3								2
cnode	8	5	4	5	14	15	3	4	5	14	15	11	12	13	2
Bus	2														1
cnode	3	4	5	14	15	11	12	13	9	10	6	7	8	1	2
Bus	1														
cnode	3	4	5	14	15	11	12	13	9	10	6	7	8		

The flowchart as shown in Fig. 11 has been developed in such a way that 'cnode' vector stores information of buses connected beyond each bus. The vectors 'bntagf(i)' and 'bntagto(i)' stores starting and ending locations in 'cnode' vector, where buses beyond bus 'i' are stored. The vectors 'cnode', 'bntagf' and 'bntagto' have been developed by extracting information of sending end and receiving end nodes of each line in RDS. The values of bntagf and bntagto for each bus in IEEE 15 bus RDS are presented in Table 27 and cnode information is presented in Table 28.

IEEE 15 bus RDS at single contingency

The flowchart as shown in Fig. 12 provides line and bus data of each part of network when a single line outage has taken place. OPF requires line data of part-II of network in order to compute scheduled load and generation. Line data information in part-I and part-II of the network are stored in LD_{sub} and LD_{ws} matrices respectively.

Line data information of part-I (LD_{sub}) and part-II (LD_{ws}) of IEEE 15 bus RDS by considering the line outage between buses 2 and 3 are shown in Tables 29 and 30 respectively.

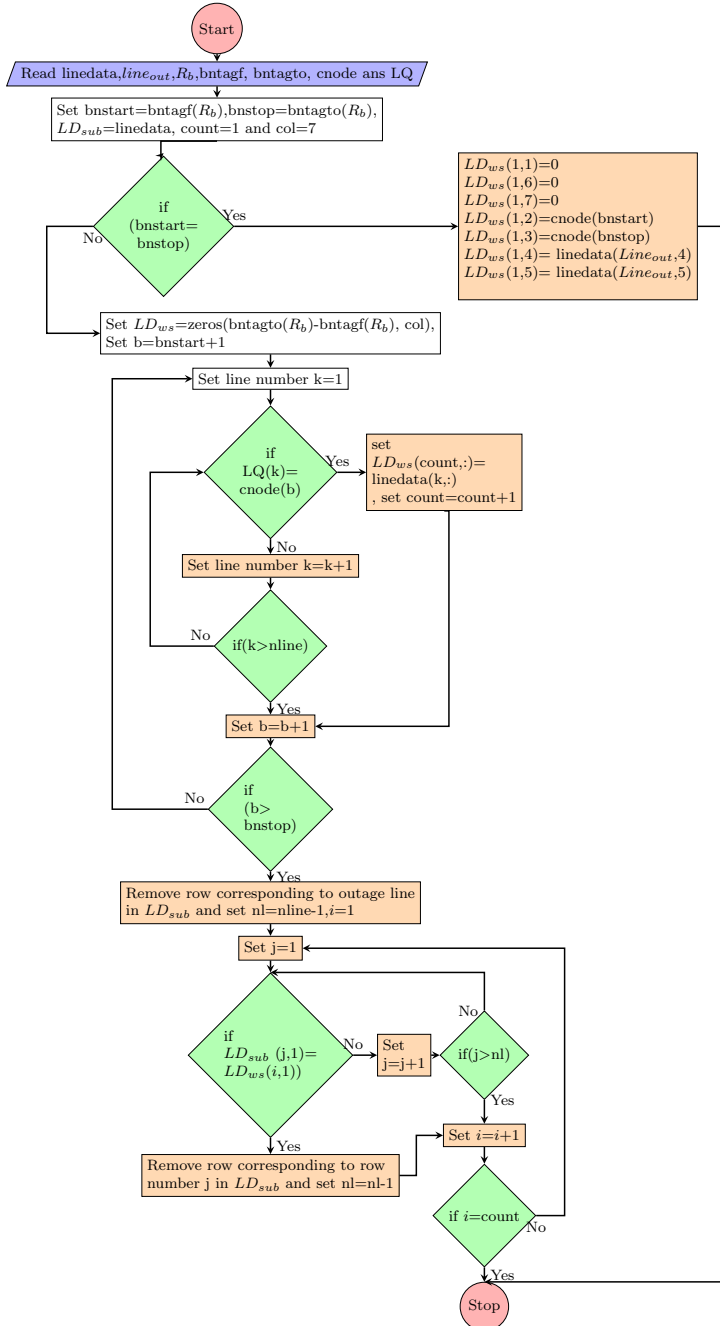


Fig. 12 Flowchart for line data selection of network at single contingency

Table 29 Line and Bus data of part-I of IEEE 15 bus RDS before renumbering after the line outage between buses 2 and 3 (LD_{sub})

Line	From	To	P(pu)	Q(pu)	R(pu)	X(pu)
1	1	2	0.2205	0.2249	0.0022	0.0022
5	2	9	0.3500	0.3570	0.0033	0.0022
7	2	6	0.7000	0.7141	0.0042	0.0029
8	6	7	0.7000	0.7141	0.0018	0.0012
9	6	8	0.3500	0.3570	0.0021	0.0014
6	9	10	0.2205	0.2249	0.0028	0.0019

Table 30 Line and Bus data of part-II of IEEE 15 bus RDS before renumbering after the line outage between buses 2 and 3 (LD_{ws})

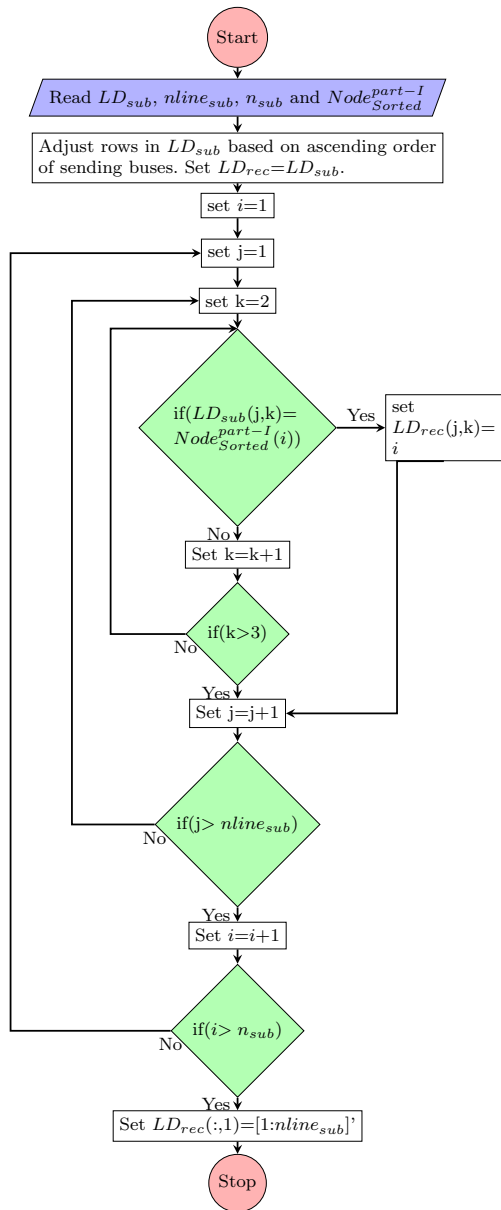
Line	From	To	P(pu)	Q(pu)	R(pu)	X(pu)
10	3	11	-0.5500	0.1087	0.0030	0.0020
14	4	15	-3.0500	-1.1021	0.0020	0.0013
4	4	5	0.2205	0.2249	0.0025	0.0017
12	12	13	0.2205	0.2249	0.0033	0.0022
13	4	14	0.3500	0.3570	0.0037	0.0025
11	11	12	0.3500	0.3570	0.0040	0.0027
3	3	4	0.7000	0.7141	0.0014	0.0014

Renumbering of buses in part-I of IEEE 15 bus RDS

Bus numbers which were stored in LD_{sub} from Fig. 12 may not be in sequence as some of buses were moved to LD_{ws} . In order to run any distribution load flow successfully on any part of network, it requires proper numbering of each line and bus. The process of renumbering of all buses in part-I of network is depicted in the flowchart as shown in Fig. 13.

Part-I of IEEE 15 bus RDS after renumbering is shown in Table 31.

Fig. 13 Flowchart for Renumbering buses in part-I of network



Identification of Slack bus and position of each bus from slack bus in part-II of IEEE 15 bus RDS

A new algorithm has been developed to identify slack bus and position of remaining buses from slack bus. In this method the bus which has highest power injection has been considered as slack bus. This method also provides information about position

Table 31 Renumbered line and Bus data of part-I of IEEE 15 bus RDS after line outage between buses 2 and 3 LD_{rec}

Line	From	To	P(pu)	Q(pu)	R(pu)	X(pu)
1	1	2	0.2205	0.2249	0.0022	0.0022
2	2	6	0.3500	0.3570	0.0033	0.0022
3	2	3	0.7000	0.7141	0.0042	0.0029
4	3	4	0.7000	0.7141	0.0018	0.0012
5	3	5	0.3500	0.3570	0.0021	0.0014
6	6	7	0.2205	0.2249	0.0028	0.0019

of remaining buses from slack bus and this information is stored in $Node_{pos}$. The flowchart as shown in Fig. 14 has employed the following logic:

- Identify the bus which has maximum injection and consider it as slack bus and keep that bus as first element in vector $Node_{pos}$
- Identify the position of each bus from slack bus in part-II of network and update $Node_{pos}$

Information about slack bus and position of remaining buses from slack bus in part-II of IEEE 15 bus RDS are shown in Tables 32. Index represents location of bus in $Node_{pos}$.

Renumbering of buses in part-II of IEEE 15 bus RDS

In order to run any distribution load flow successfully on part-II of network, proper numbering of each line and bus is required. The flowchart as shown in Fig. 15 is employed for renumbering the line and buses in part-II of network. Part-II of IEEE 15 bus RDS after renumbering is shown in Table 33.

The basic logic used for renumbering the buses and lines in part-II of network is as follows:

- Identify sending end and receiving end buses of each line of part-II of network (LD_{ws}^{ren}).
- If any of these two buses exist in $Node_{pos}$, then replace that bus number in LD_{ws}^{ren} with index of that bus in $Node_{pos}$ matrix.

Flowchart for computing LMP using HGDA-OPF

Flowchart of the proposed HGDA-OPF method to compute LMP value of each DG unit in part-II of network based on reliability improvement and also to observe the state of the network connected to the substation is presented in Fig. 16.

Fig. 14 Flowchart for Slack bus and position of each bus from slack bus in part-II of network

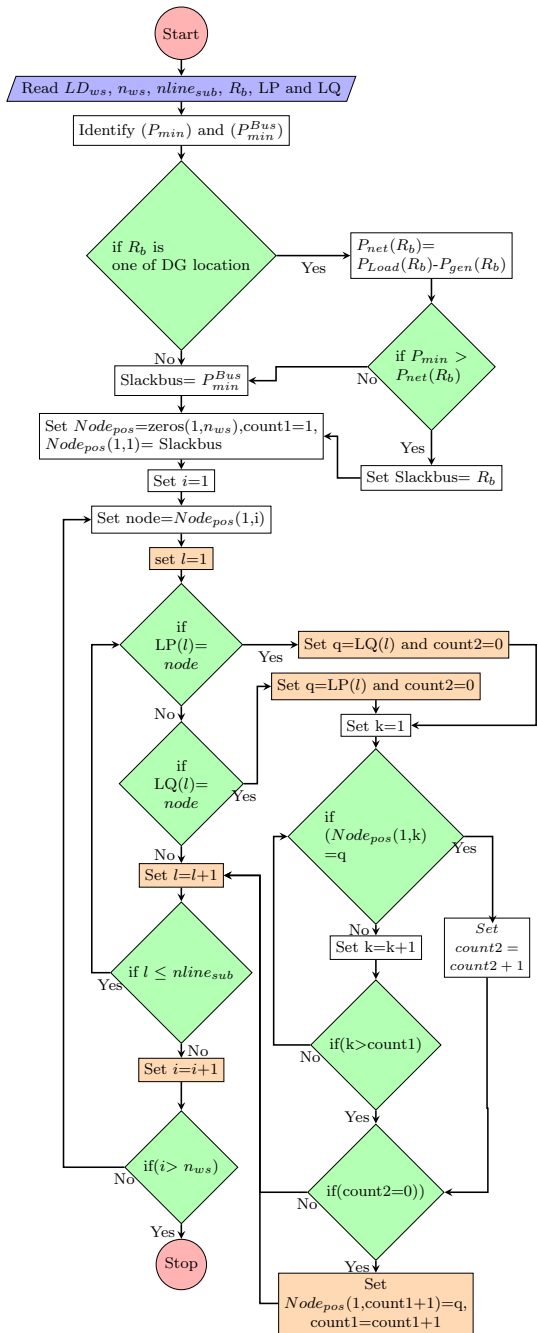


Table 32 $Node_{pos}$ matrix

Index	1 (Slack bus)	2	3	4	5	6	7	8
$Node_{pos}$	15	4	3	5	14	11	12	13

Fig. 15 Flowchart for
Renumbering of buses in part-II
of network

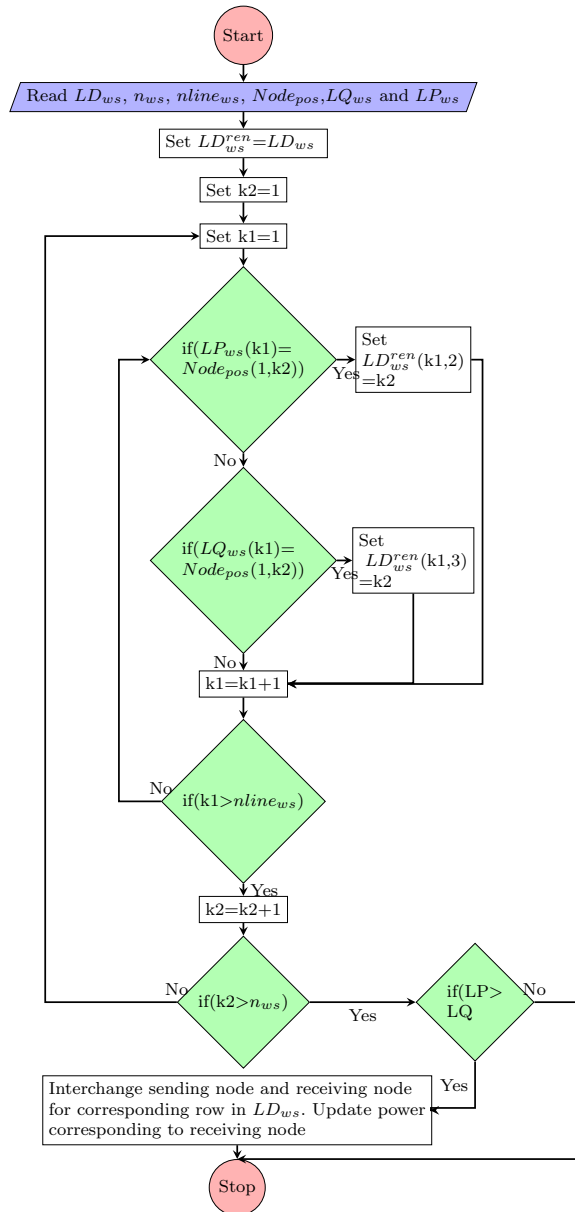


Table 33 Renumbered line and bus data of part-II of IEEE 15 bus RDS after the line outage between buses 2 and 3 (LD_{ws}^{ren})

Line	From	To	P(pu)	Q(pu)	R(pu)	X(pu)
1	1	2	0.7000	0.7141	0.0020	0.0013
2	2	4	0.2205	0.2249	0.0025	0.0017
3	2	5	0.3500	0.3570	0.0037	0.0025
4	2	3	0.7000	0.7141	0.0014	0.0014
5	3	6	-0.5500	0.1087	0.0030	0.0020
6	6	7	0.3500	0.3570	0.0040	0.0027
7	7	8	0.2205	0.2249	0.0033	0.0022

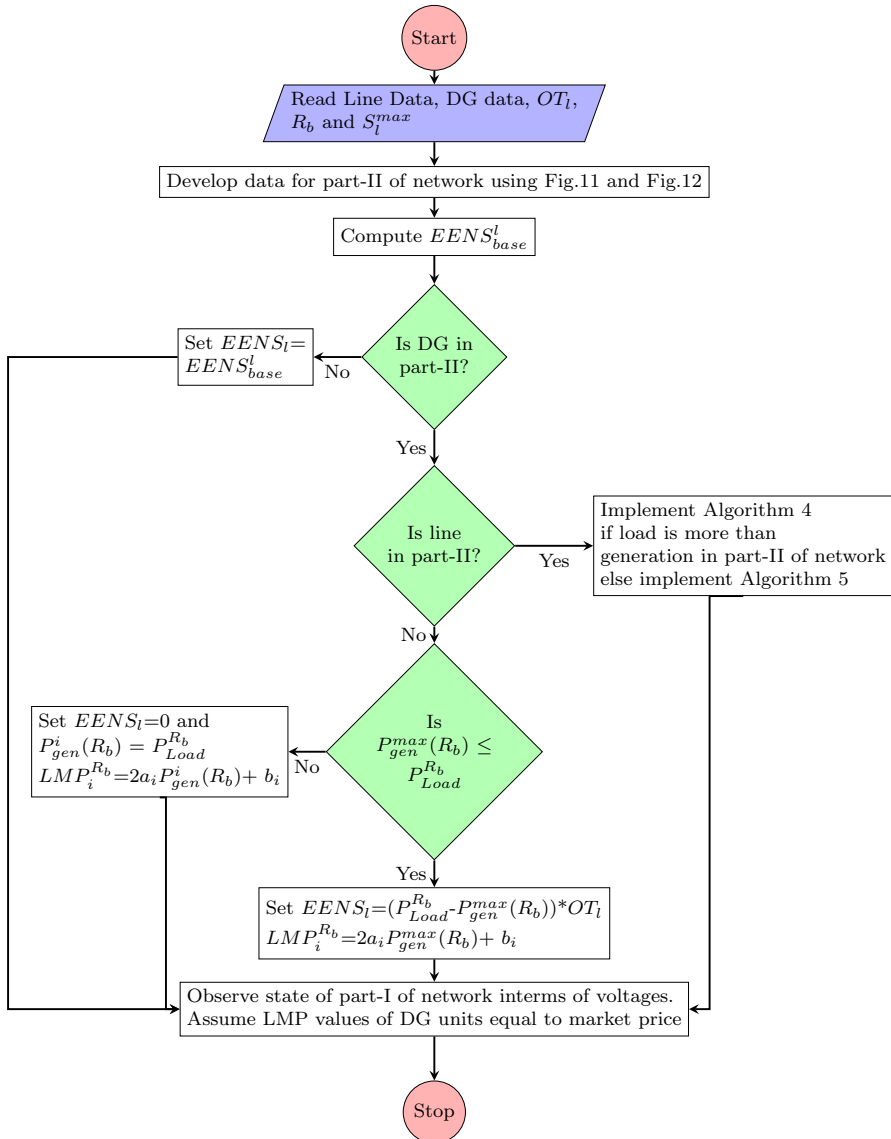


Fig. 16 Flowchart for computation of LMP at DG buses

References

1. Kavousifard, A., Samet, H.: Consideration effect of uncertainty in power system reliability indices using radial basis function network and fuzzy logic theory. *Neurocomputing* **74**(17), 3420–3427 (2011)
2. Allan, R.N., Billinton, R., Sjariel, I., Goel, L., So, K.: A reliability test system for educational purposes–basic distribution system data and results. *IEEE Trans. Power Syst.* **6**(2), 813–820 (1991)
3. Billinton, R., Allan, R.N.: Reliability evaluation of power systems, 2nd edn. Plenum, New York (1996)

4. Kavousi-Fard, A., Niknam, T.: Optimal distribution feeder reconfiguration for reliability improvement considering uncertainty. *IEEE Trans. Power Deliv.* **29**(3), 1344–1353 (2014)
5. Madani, V., Das, R., Aminifar, F., McDonald, J., Venkata, S., Novosel, D., Bose, A., Shahidehpour, M.: Distribution automation strategies challenges and opportunities in a changing landscape. *IEEE Trans. Smart Grid* **6**(4), 2157–2165 (2015)
6. Ziari, I., Ledwich, G., Ghosh, A., Platt, G.: Integrated distribution systems planning to improve reliability under load growth. *IEEE Trans. Power Deliv.* **27**(2), 757–765 (2012)
7. Kavousi-Fard, A., Akbari-Zadeh, M.-R.: Reliability enhancement using optimal distribution feeder reconfiguration. *Neurocomputing* **106**, 1–11 (2013)
8. Etemadi, A., Fotuhi-Firuzabad, M.: Distribution system reliability enhancement using optimal capacitor placement. *IET Gener. Transm. Distrib.* **2**(5), 621–631 (2008)
9. Donadel, C.B., Fardin, J.F., Encarnação, L.F.: Electrical distribution network operation with a presence of distributed generation units in a pre smart grid environment using a clustering-based methodology. *Energy Syst.* **6**(4), 455–477 (2015)
10. Vita, V., Ekonomou, L., Christodoulou, C.A.: The impact of distributed generation to the lightning protection of modern distribution lines. *Energy Syst.* **7**(2), 357–364 (2016)
11. Photovoltaics, D.G., Storage, E.: Ieee guide for design, operation, and integration of distributed resource island systems with electric power systems.(2011)
12. Awad, A.S., El-Fouly, T.H., Salama, M.M.: Optimal ess allocation and load shedding for improving distribution system reliability. *IEEE Trans. Smart Grid* **5**(5), 2339–2349 (2014)
13. Farsani, E.A., Abyaneh, H.A., Abedi, M., Hosseiniyan, S.: A novel policy for lmp calculation in distribution networks based on loss and emission reduction allocation using nucleolus theory. *IEEE Trans. Power Syst.* **31**(1), 143–152 (2016)
14. Sotkiewicz, P.M., Vignolo, J.M.: Nodal pricing for distribution networks: efficient pricing for efficiency enhancing dg. *IEEE Trans. Power Syst.* **21**(2), 1013 (2006)
15. Shaloudegi, K., Madinehi, N., Hosseiniyan, S., Abyaneh, H.A.: A novel policy for locational marginal price calculation in distribution systems based on loss reduction allocation using game theory. *IEEE Trans. Power Syst.* **27**(2), 811–820 (2012)
16. Algarni, A.A., Bhattacharya, K.: A generic operations framework for discos in retail electricity markets. *IEEE Trans. Power Syst.* **24**(1), 356–367 (2009)
17. Sotkiewicz, P.M., Vignolo, J.M.: Towards a cost causation-based tariff for distribution networks with dg. *IEEE Trans. Power Syst.* **22**(3), 1051–1060 (2007)
18. Sathyaranayana, B.R., Heydt, G.T.: Sensitivity-based pricing and optimal storage utilization in distribution systems. *IEEE Trans. Power Deliv.* **28**(2), 1073–1082 (2013)
19. Singh, R.K., Goswami, S.: Optimum allocation of distributed generations based on nodal pricing for profit, loss reduction, and voltage improvement including voltage rise issue. *Int. J. Electr. Power Energy Syst.* **32**(6), 637–644 (2010)
20. Azad-Farsani, E., Askarian-Abyaneh, H., Abedi, M., Hosseiniyan, S.H.: Stochastic locational marginal price calculation in distribution systems using game theory and point estimate method, yIET Generation. Transm. Distrib. **9**(14), 1811–1818 (2015)
21. Azad-Farsani, E., Agah, S., Askarian-Abyaneh, H., Abedi, M., Hosseiniyan, S.: Stochastic lmp (locational marginal price) calculation method in distribution systems to minimize loss and emission based on shapley value and two-point estimate method. *Energy* **107**, 396–408 (2016)
22. Chowdhury, A.A., Koval, D.O.: Current practices and customer value-based distribution system reliability planning. *IEEE Trans. Ind. Appl.* **40**(5), 1174–1182 (2004)
23. Resener, M., Haffner, S., Pereira, L.A., Pardalos, P.M.: Mixed-integer lp model for volt/var control and energy losses minimization in distribution systems. *Electr. Power Syst. Res.* **140**, 895–905 (2016)
24. Gonçalves, R.R., Franco, J.F., Rider, M.J.: Short-term expansion planning of radial electrical distribution systems using mixed-integer linear programming. *IET Gener. Transm. Distrib.* **9**(3), 256–266 (2014)
25. Ganguly, S., Sahoo, N., Das, D.: A novel multi-objective pso for electrical distribution system planning incorporating distributed generation. *Energy Syst.* **1**(3), 291–337 (2010)
26. Kao, Y.-T., Zahara, E.: A hybrid genetic algorithm and particle swarm optimization for multimodal functions. *Appl. Soft Comput.* **8**(2), 849–857 (2008)
27. Mirjalili, S.: Dragonfly algorithm: a new meta-heuristic optimization technique for solving single-objective, discrete, and multi-objective problems. *Neural Comput. Appl.* **27**(4), 1053–1073 (2016)

28. Frank, S., Steponavice, I., Rebennack, S.: Optimal power flow: a bibliographic survey i. *Energy Syst.* **3**(3), 221–258 (2012)
29. Mitra, J., Vallem, M.R., Singh, C.: Optimal deployment of distributed generation using a reliability criterion. *IEEE Trans. Ind. Appl.* **52**(3), 1989–1997 (2016)
30. Schuerger, R., Harris, R.A., Dowling, N.: Why existing utility metrics do not work for industrial reliability analysis. *IEEE Trans. Ind. Appl.* **52**(4), 2801–2806 (2016)
31. Narimani, M.R., Vahed, A.A., Azizipanah-Abarghooee, R., Javidsharifi, M.: Enhanced gravitational search algorithm for multi-objective distribution feeder reconfiguration considering reliability, loss and operational cost. *IET Gener. Transm. Distrib.* **8**(1), 55–69 (2014)
32. Shirmohammadi, D., Hong, H., Semlyen, A., Luo, G.: A compensation-based power flow method for weakly meshed distribution and transmission networks. *IEEE Trans. Power Syst.* **3**(2), 753–762 (1988)
33. Abdel-Akher, M.: Voltage stability analysis of unbalanced distribution systems using backward/forward sweep load-flow analysis method with secant predictor. *IET Gener. Transm. Distrib.* **7**(3), 309–317 (2013)
34. Wang, Z., Chen, F., Li, J.: Implementing transformer nodal admittance matrices into backward/forward sweep-based power flow analysis for unbalanced radial distribution systems. *IEEE Trans. Power Syst.* **19**(4), 1831–1836 (2004)
35. Moghaddas-Tafreshi, S., Mashhour, E.: Distributed generation modeling for power flow studies and a three-phase unbalanced power flow solution for radial distribution systems considering distributed generation. *Electr. Power Syst. Res.* **79**(4), 680–686 (2009)
36. Goldberg, D.E., Holland, J.H.: Genetic algorithms and machine learning. *Mach. Learn.* **3**(2), 95–99 (1988)
37. Devaraj, D., Yegnanarayana, B.: Genetic-algorithm-based optimal power flow for security enhancement. *IEE Proc. Gener. Transm. Distrib.* **152**(6), 899–905 (2005)
38. Deb, K.: An introduction to genetic algorithms. *Sadhana* **24**(4–5), 293–315 (1999)
39. Deb, K., Deb, D.: Analysing mutation schemes for real-parameter genetic algorithms. *Int. J. Artif. Intell. Soft Comput.* **4**(1), 1–28 (2014)
40. Yang, X.-S.: *Nature-Inspired Optimization Algorithms*. Elsevier, Amsterdam (2014)
41. Juang, C.-F.: A hybrid of genetic algorithm and particle swarm optimization for recurrent network design. *IEEE Trans. Syst. Man Cybernet. Part B (Cybernet.)* **34**(2), 997–1006 (2004)
42. Ks, S.R., Murugan, S.: Memory based hybrid dragonfly algorithm for numerical optimization problems. *Expert Syst. Appl.* **83**, 63–78 (2017)
43. Release, M.: *The mathworks, Inc.*, Natick, vol. 488 (2013)
44. Singh, D., Misra, R.: Effect of load models in distributed generation planning. *IEEE Trans. Power Syst.* **22**(4), 2204–2212 (2007)
45. Rao, R.S.: Capacitor placement in radial distribution system for loss reduction using artificial bee colony algorithm. *Int. J. Eng. Nat. Sci.* **4**(2), 84–88 (2010)
46. Das, D., Kothari, D., Kalam, A.: Simple and efficient method for load flow solution of radial distribution networks. *Int. J. Electr. Power Energy Syst.* **17**(5), 335–346 (1995)
47. Murthy, K.R., Raju, M.R., Rao, G.G., Rao, K.N.: Topology based approach for efficient load flow solution of radial distribution networks. In: 16th National Power Systems Conference, pp. 176–219 (2010)